Published by
NIGERIAN SOCIETY OF PHYSICAL SCIENCES
Available online @ https://journal.nsps.org.ng/index.php/jnsps

J. Nig. Soc. Phys. Sci. 7 (2025) 2732

Journal of the Nigerian Society of Physical Sciences

Modeling the dynamics of pertussis to assess the influence of timely awareness with optimal control analysis

J. Andrawus[a,*], J. Y. Musa[a], S. Babuba[a], A. Yusuf[a,b,c], S. Qureshi[d,e,f], U. T. Mustapha[a], O. Akpodamure[g], I. S. Mamba[h]

[a]*Department of Mathematics, Federal University Dutse, 7156, Nigeria*
[b]*Department of Mathematics, Firat University, Elazig, Turkey*
[c]*Department of Mathematics, Saveetha School of Engineering, Saveetha Institute of Medical and Technical Sciences, Saveetha University, Chennai 602105*
[d]*Department of Basic Sciences and Related Studies, Mehran University of Engineering & Technology, Jamshoro – 76062, Pakistan*
[e]*Department of Mathematics, Near East University, 99138, Mersin, Turkey*
[f]*Research Center of Applied Mathematics, Khazar University Baku, Azerbaijan*
[g]*Department of Statistics, Federal Polytechnic Orogun, Delta State, Nigeria*
[h]*Department of Mathematics, Ibrahim Badamassi Babangida University Lapai, Niger State, Nigeria*

Abstract

Pertussis, also known as whooping cough, is a very infectious respiratory disease that can be easily avoided with vaccination. In this work, a system of nonlinear ordinary differential equations of pertussis has been formulated to examine the impact of early treatment. Through theoretical examination, the model has been extensively analyzed. Numerical experiments are performed to validate the theoretical conclusions. The suggested model has been fitted to real Austrian pertussis data, demonstrating that it is appropriate for the data. The control reproduction number was also used to test the sensitivity analysis of all of the parameters of the proposed model. The results indicate that the effective contact rate is the parameter that is more sensitive to increasing the control reproduction number. In contrast, the awareness rate is the parameter that is most sensitive to decreasing the number of control reproductions, and optimal control analysis has also been performed in this work. Numerical simulation reveals that awareness is the most influential parameter in reducing infection in the population. Moreover, vaccination and treatment are also very important in controlling pertussis in society.

DOI:10.46481/jnsps.2025.2732

Keywords: Dynamics, Optimal control, Mathematical model, Control reproduction number, Pertussis

Article History :
Received: 06 March 2025
Received in revised form: 21 May 2025
Accepted for publication: 23 May 2025
Published: 18 August 2025

Communicated by: Pankaj thakur

1. Introduction

Pertussis is a very infectious respiratory disease that can be readily avoided with vaccination. For newborns, whooping cough poses an especially serious risk [1]. In addition to a "whoop"-like cough, other symptoms include sneezing, nasal congestion, and a runny nose. Bordetella pertussis is the bacterium that causes pertussis, also known as whooping cough. The disease mainly affects the upper respiratory system and is extremely contagious [1]. Worldwide, whooping cough, also

*Corresponding author Tel. No: +234-806-783-6348.
Email address: james.a@fud.edu.ng (J. Andrawus)

known as pertussis, is a major cause of infant mortality and a public health problem, even in nations with high immunisation rates [2]. Infants under 12 months old who have not received all or some vaccinations account for most reported deaths. However, adults and teenagers are also infected by the disease [3].WHO estimates that each year there are between 40 and 50 million whooping cough infections, with 297,000 to 409,000 deaths. Ninety per cent of cases occur in low-income countries [4]. There were 24.1 million cases of pertussis worldwide in 2014, according to a report. This disease claimed the lives of almost 160,700 children under five years of age [5, 6]. It was in France in 1578 that the first outbreak was observed. 107 people died in Cape Town during a significant whooping cough outbreak in 1947 [7]. In the 1600s, it was widespread throughout other European countries [4]. Before vaccination was introduced in England and Wales in 1957, there were about 100,000 documented cases of pertussis each year [8]. In early 2010, there was an outbreak in Israel, the United States, and Ireland. 2014 saw the highest whooping cough outbreak since 1947, with more than 10,000 confirmed cases in California [7].

Whooping cough bacteria are easily transmitted from person to person through the air [11]. An infected person may cough or sneeze and release tiny particles that contain bacteria [9]. The germs are then inhaled by other people [9]. In addition, it spreads when individuals interact often or share breathing spaces, such as when a newborn is carried on your chest [9]. After infection, the first symptoms usually show up seven to ten days later. They consist of a low-grade fever, a runny nose, and a cough, which usually progresses to a hacking cough and whooping (hence the term whooping cough). Pneumonia is a fairly common consequence, but brain damage and convulsions are uncommon [10].

Antibiotics can be useful, but supportive care is the mainstay of medical therapy for instances of pertussis [10]. This treatment removes the organism from secretions, which reduces communicability and, if started early, changes the way the disease progresses. Erythromycin, clarithromycin, and azithromycin are suggested antibiotics [11]. You can also use trimethoprim-sulfamethoxazole [11]. Regardless of age or immunisation status, all close contacts of a person with pertussis should receive an antibiotic that is effective against the disease [11]. Vaccination is the main method of controlling pertussis. Mass immunisation began with the introduction of diphtheria-tetanus-pertussis (DTP) as the primary vaccine in the first year of life in several countries throughout the 1950s. The incidence of illness and death has decreased by more than 90% [12]. WHO recommends giving the first dose as early as six weeks of age and then giving the second and third doses at intervals of four to eight weeks, or ages ten to fourteen and fourteen to eighteen weeks. Preferably, in the second year of life, a booster dose is advised. More booster doses might be necessary later in life, depending on the local epidemiology [10].

Several researchers developed a mathematical model to study the transmission dynamics of pertussis using various control measures among these: a study by Ref. [7] recommended that the best control method would be to combine vaccination and quarantine to prevent the spread of whooping cough. A study by Ref. [13] indicated that the change in epidemiological observations in Australia during the analysis period is compatible with the selective pressure of acellular pertussis vaccination. In the research by Ref. [14, 15], a mathematical model of pertussis was formulated; they found that the length and intensity of the outbreaks are highly influenced by the timing of contact tracing. The study by Ref. [16] stated that in order to reduce the severity and prevalence of the disease, a booster vaccination program could be more beneficial than a single immunisation campaign. Furthermore, the study by Refs. [17] indicated that a decrease in the duration of protection after vaccination due to a change in the pathogen is the most likely factor to account for the 1996-1997 epidemic. Optimal control theory is a branch of control theory that deals with finding a control for a dynamical system over a period of time such that an objective function is optimised. It has numerous applications in science, engineering, and operations research. Ref. [18] formulated a mathematical model within an optimal control framework of a generic disease, accounting for treatment and media reporting of disease-induced deaths, their study analyzes the effect of different incidence functions on disease transmission, and the qualitative nature of epidemic dynamics by performing optimal control analysis using three different contact rates and a media function that is dependent on the number of deaths. However, the optimal control in this work focuses on awareness by providing health education.

Considering all the research mentioned above, Refs. [7, 13, 15–17]. The fact that none of the above-mentioned authors considered timely awareness was specifically motivated by the work of Ref. [17], which also did not consider timely awareness. We developed a mathematical model of pertussis (whooping cough) considering aware susceptible and unaware susceptible, this is indeed important in the dynamics of pertussis and also, we considered three different kinds of vaccination administration:

- It can be administered at recruitment,
- It can be administered by awareness, and
- both the two cases stated earlier can be given booster vaccinated.

We also considered the evaluation of the influence of vaccinations, timely awareness, and treatment in some compartments.

The organization of the paper is as follows. Section 1, contain the introduction and pertinent literature, section 2 covers the formulation of the model, section 3 covers the analytical analysis of the model, Section 5 contains optimal control analysis, section 4 covers the model fittings and sensitivity analysis of the control reproduction number, section 6 covers numerical simulations associated with the model, and Section 7 covers the concluding remarks and recommendation.

2. Model Description

The model divided the human population at time t into six subgroups: Susceptible, Unvaccinated people $S_u(t)$, this group

consists of those individuals who are at risk of infection. Susceptible vaccinated $S_v(t)$, this group consists of all individuals who take the vaccine, however, some can get the infection at a slower rate. Exposed $E(t)$ refers to $S_u(t)$ and $S_v(t)$ that make effective contact with infectious individuals. infected individual $I(t)$, this group refers to all infected individuals. An infected individual under treatment $I_t(t)$, this group consists of all individuals under treatment, and Recovered $R(t)$, this group consists of individuals who recover naturally and due to treatment. The susceptible un-vaccinated group is recruited by $\Pi(1-P_1)$, and the group increases with the waning rate of vaccine ω, it decreases by the natural mortality rate μ, and it further decreases by the rate of infection λ. The susceptible vaccinated group is recruited by Πp_1; the group is generated by the coverage of vaccine due to awareness p_1; it decreases by the recovery rate due to booster vaccination p_3 and the natural mortality rate μ; and it further decreases by the rate $(1-\theta)\lambda$, where $(1-\theta)(0 < (1-\theta) < 1)$ is the risk of infectiousness reduction of vaccinated individuals. The exposed group is generated by λ and $(1-\theta)\lambda$; it decreases with the progression rate and treatment due to awareness of the exposed individuals σ and γ_1. The infected group is generated by $\sigma(1-\gamma_1)$, and decreases with treatment due to awareness of the infectious individuals. γ_2, it also decreases by the natural recovery rate α, and it further decreases by the natural mortality rates μ and the mortality rate due to infection δ. Infected individuals in the treatment group are generated by γ_2; it decreases by the recovery rate due to treatment τ; it also decreases by μ. Recovered groups are generated by the recovery rate due to booster vaccination p_3; it also increases by τ and decreases by the natural mortality rate μ. Consequently, the entire human population at any given moment t is given by

$$N(t) = S_u(t) + S_v(t) + E(t) + I(t) + I_t(t) + R(t). \tag{1}$$

$$\begin{aligned}
\frac{dS_u}{dt} &= \Pi(1-p_1) + \omega S v - \lambda S_u - (\mu + p_2)S_u,\\
\frac{dS_v}{dt} &= \Pi p_1 + p_2 S_u - (1-\theta)\lambda S_v - (\omega + \mu + p_3)S_v,\\
\frac{dE}{dt} &= \lambda S_u + (1-\theta)\lambda S_v - (\mu+\sigma)E,\\
\frac{dI}{dt} &= \sigma(1-\gamma_1)E - (\mu + \delta + \alpha + \gamma_2)I,\\
\frac{dI_t}{dt} &= \sigma\gamma_1 E + \gamma_2 I - (\mu+\tau)I_t,\\
\frac{dR}{dt} &= p_3 S_v + \alpha I + \tau I_t - \mu R,
\end{aligned} \tag{2}$$

where

$$\lambda = \frac{(1-\epsilon)\beta(I+\eta I_t)}{N} \tag{3}$$

3. Analytical analysis of the model

3.1. Positivity and boundedness of solutions

The theoretical framework deals with the human population. It is now possible to demonstrate that for any $t \geq 0$, all state variables in the model (2) are non-negative.

Theorem. A dynamical system in the closed set defined by the equation 2 is provided by

$$\Omega = \{(S_u(t), S_v(t), E(t), I(t), I_t(t), R(t)) \in \mathbf{R}_+^6 : N \leq \frac{\pi}{\mu}\}. \tag{4}$$

Proof. Here, we need to demonstrate the positive invariance of R_+^6, that is, no solution to the system 2 that is in Ω exits Ω (Theorem 2.1.5) of Ref. [19]). Assume that $R(0)) > 0$ and that $S_u(0), S_v(0), E(0), I(0), and I_t(0) > 0$. If $S_u(0)$ and $S_v(0)$ are not both positive, then $S_u(t) > 0$ and $S_v(t) > 0$ for $t \in [0, \tilde{t})$ exist at some time $\tilde{t} > 0$ and $S_u(\tilde{t}) = S_v(\tilde{t}) = 0$. Using second, third, fourth, and fifth equations, we now get,

$$\begin{aligned}
\frac{dE(t)}{dt} &\geq -(\mu+\sigma)E(t) \quad \text{for} \quad t \in [0, \tilde{t}),\\
\frac{dI(t)}{dt} &\geq -(\mu+\delta+\alpha+\gamma_2)I(t) \quad \text{for} \quad t \in [0, \tilde{t}),\\
\frac{dI_t(t)}{dt} &\geq -(\mu+\tau)I_t(t) \quad \text{for} \quad t \in [0, \tilde{t}).
\end{aligned} \tag{5}$$

Consequently, $E(0) > 0, I(0) > 0$ and $I_t(0) > 0$ for $t \in [0, \tilde{t})$. As a result, using the system 2's first and second equations, we've obtained

$$\frac{dS_u(t)}{dt} \geq -(p_2+\mu+\lambda)S_u(t) \quad \text{for} \quad t \in [0, \tilde{t}),$$

$$\frac{dS_v(t)}{dt} \geq -(\mu+\omega+p_3+(1-\theta)\lambda)S_v(t) \quad \text{for} \quad t \in [0, \tilde{t}).$$

One can see that, $S_u(0) > 0$ and $S_v(0) > 0$ which contradict our assumption of $S_u(\tilde{t}) = S_v(\tilde{t}) = 0$. Hence $S_u(t)$ and $S_v(t)$ are positive. Conversely, a subsystem of (2) that does not include the first and second equations may be expressed in matrix form as follows, demonstrating the positivity of the model's remaining state variable.

$$\frac{dX(t)}{dt} = \mathcal{M}Y(t) + B(t), \tag{6}$$

with

$$\begin{aligned}
Y(t) &= \begin{pmatrix} E, & I, & I_t, & R \end{pmatrix}^T,\\
\mathcal{M} &= \begin{pmatrix} -k_3 & k & \eta k & 0\\ \sigma(1-\gamma_2) & -k_4 & 0 & 0\\ \sigma\gamma_1 & \gamma_2 & -k_5 & 0\\ 0 & \alpha & \tau & -\mu \end{pmatrix},\\
B(t) &= \begin{pmatrix} 0 & 0 & 0 & 0 \end{pmatrix}^T,
\end{aligned} \tag{7}$$

where, $k = \beta(1-\epsilon)\frac{S_u+(1-\theta)S_v}{N}$, $k_3 = \mu+\sigma$, $k_4 = \mu+\delta+\alpha+\gamma_2$ and $k_5 = \tau+\mu$, The fact that both $S_u(t)$ and $S_v(t)$ are non-negative indicates that $\mathcal{M}$ is a Metzler matrix. indicating that subsystem (6) is a monotone system [20]. Therefore, under the flow of subsystem (6), $\mathbb{R}_+^4$ is invariant. $\mathbb{R}_+^6$ consequently becomes positively invariant under the system's flow (2). Furthermore, we need to prove the total population of humans at time t, $N(t)$ satisfies the boundedness property $0 \leq N(t) \leq \frac{\Pi}{\mu}$ whenever $0 \leq N(0) \leq \frac{\Pi}{\mu}$. We point out that this bound represents the unique equilibrium of the dynamics of the total population in

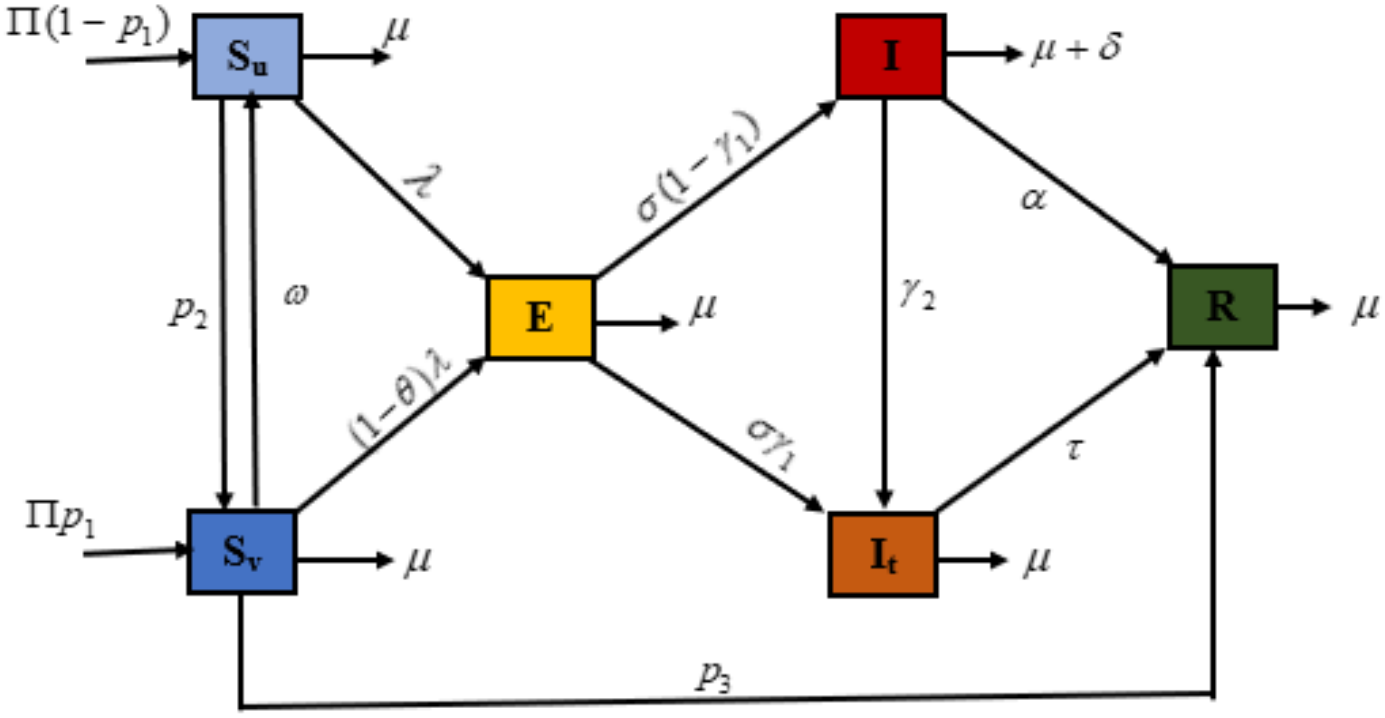

Figure 1. Model (2) diagrammatical description.

Table 1. Interpretation of the state variables and parameters used in the model (2).

Variable	Description
N	Total population at time, t
S_u	Susceptible un-vaccinated individuals at time, t
S_v	Susceptible vaccinated individuals at time, t
E	Exposed individuals at time, t
I	Infected individuals at time, t
I_t	Infected individuals under treatment at time, t
R	Recovered individuals at time, t
Parameter	**Description**
Π	Recruitment rate
p_1	Vaccination of recruitment
p_2	Vaccination due to awareness
p_3	Vaccination booster
ω	Reversion rate
μ	Natural mortality rate
β	Effective contact rate
$(1-\theta)$	Reduction rate of infection due to vaccine
γ_1	Treatment due to awareness of the exposed individuals
γ_2	Treatment due to awareness of the infectious individuals
δ	Mortality rate due to infection
α	Natural recovery rate
σ	Progression rate
ϵ	Awareness rate
τ	Recovery rate due to treatment
η	modification parameter due to reduced of the infectiousness of infected individuals under treatment

the ideal situation where there are no ongoing pertussis cases. By adding the equation of model (2), one obtains the conservation law [21]. We focused on showing that any solution in Ω remains in Ω. Therefore, the rate of change of total population is given by,

$$\frac{dN}{dt} = \Pi - \mu N - \delta I \leq \pi - \mu N. \tag{8}$$

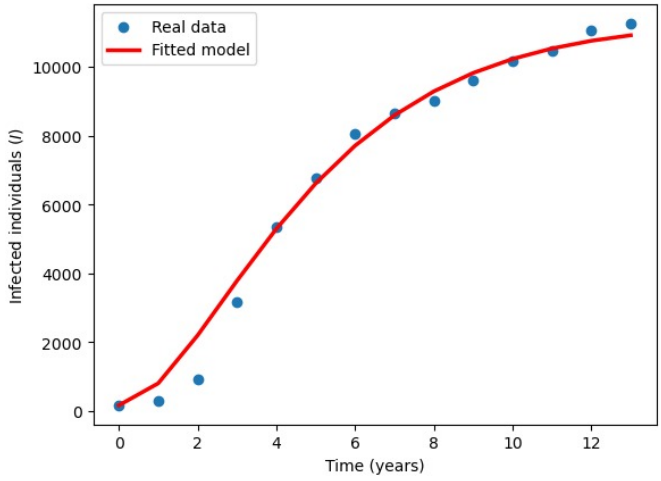

Figure 2. Comparison of real data of the disease with the simulations obtained with the proposed model.

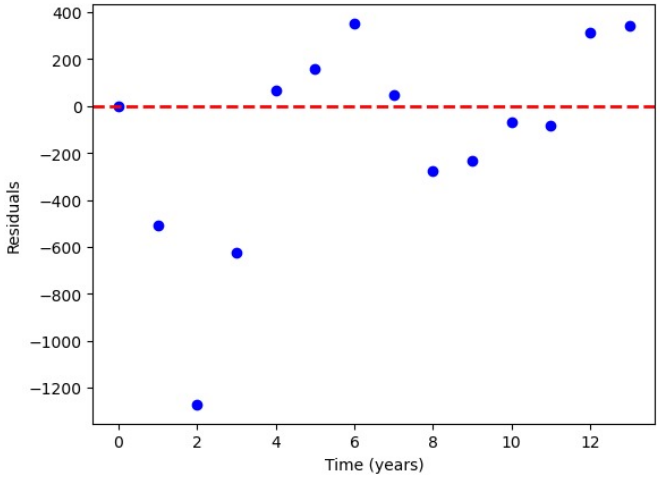

Figure 3. A depiction of the residuals for the least-squares method on the proposed model.

Applying the Groomwall inequality to equation (8), gives

$$N(t) \leq \frac{\Pi}{\mu} + \left[N(0) - \frac{\Pi}{\mu}\right] e^{-\mu t}, \forall t \geq 0, \tag{9}$$

which implies that $0 \leq N(t) \leq \frac{\Pi}{\mu}$ whenever $0 \leq N(0) \leq \frac{\Pi}{\mu}$ $\forall t \geq 0$ in another words, from equation (9), as $t \to 0$, $N(t) \to N(0) \Rightarrow N(t) \leq \frac{\Pi}{\mu}$, and as $t \to \infty$ $N(t) \to \frac{\Pi}{\mu}$. Therefore, Ω is positively invariant and a global attractor of all positive solutions of the system (2) for all positive initial conditions.

3.2. *Disease-free equilibrium and basic reproduction number*

The model system 2 possesses a disease-free equilibrium, which may be ascertained by bringing both of the equation's right-hand sides to zero and solving simultaneously to give.

$$\begin{aligned}\epsilon^0 &= (S_u^0, S_v^0, E^0, I^0, I_t^0, R^0) \\ &= \Big(\frac{\Pi((1-p_1)k_2 + \omega p_1)}{k_1 k_2 - \omega p_2}, \frac{\Pi((1-p_1)p_2 + p_1 k_1)}{k_1 k_2 - \omega p_2}, 0, 0, 0, \\ &\quad \frac{p_3 \Pi((1-p_1)p_2 + k_1 p_1)}{\mu(k_1 k_2 - \omega p_2)}\Big)\end{aligned} \tag{10}$$

where

$$k_1 = \mu + p_2, k_2 = \omega + p_3 + \mu. \tag{11}$$

3.3. *Basic reproduction number*

When an infected person interacts with a fully susceptible population in the absence of vaccination and awareness, the number of new infections they cause is known as the basic reproduction number (represented by $R_0 = \rho(FV^{-1})$ in the model 2. Here, ρ represents the spectral radius of the next-generation matrix, FV^{-1}). The stability of the equilibrium is established using the next-generation matrix technique [22–25]. The new infection terms are represented by the matrix F, while the existing transition terms are represented by the matrix V, R_0.

$$F = \begin{bmatrix} 0 & \frac{\beta(1-\epsilon)\left(S_u{}^0 + (1-\theta)S_v{}^0\right)}{N^0} & \frac{\beta\eta(1-\epsilon)\left(S_u{}^0 + (1-\theta)S_v{}^0\right)}{N^0} \\ 0 & 0 & 0 \\ 0 & 0 & 0 \end{bmatrix}, \tag{12}$$

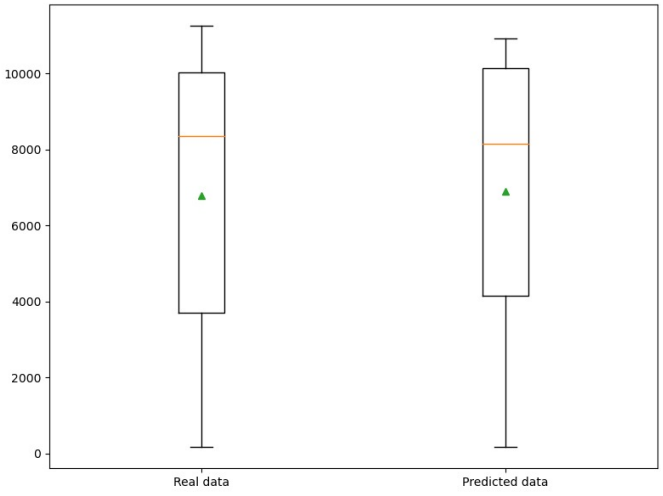

Figure 4. Statistical illustration of the real data and the model's predicted values via a box and whisker plot.

and

$$V = \begin{bmatrix} k_3 & 0 & 0 \\ -\sigma(1-\gamma_1) & k_4 & 0 \\ -\sigma\gamma_1 & -\gamma_2 & k_5 \end{bmatrix}, \tag{13}$$

$$V^{-1} = \begin{bmatrix} {k_3}^{-1} & 0 & 0 \\ -\frac{\sigma(-1+\gamma_1)}{k_3 k_4} & {k_4}^{-1} & 0 \\ \frac{\sigma((1-\gamma_1)\gamma_2 + k_4\gamma_1)}{k_3 k_4 k_5} & \frac{\gamma_2}{k_4 k_5} & {k_5}^{-1} \end{bmatrix}, \tag{14}$$

$$FV^{-1} = \begin{bmatrix} \frac{-(1-\epsilon)\beta\left(\left((k_4-\gamma_2)\eta - k_5)\gamma_1\right) + \eta\gamma_2 + k_5\right)\left(S_u^0 + (1-\theta)S_v^0\right)\sigma}{N^0 k_3 k_4 k_5} & \frac{-(1-\epsilon)\beta(S_u^0 + (1-\theta)S_v^0)(\eta\gamma_2 + k_5)}{N^0 k_4 k_5} & \frac{(1-\epsilon)\beta\eta(S_u^0 + (1-\theta)S_v^0)}{N^0 k_5} \\ 0 & 0 & 0 \\ 0 & 0 & 0 \end{bmatrix}$$

The control reproduction number $\mathcal{R}_c$ is the total number of secondary infections produced by a single individual throughout his/her

Table 2. Ranges and baseline values of parameters of model (2).

Parameter	Value	Unit	Reference	Parameter	Value	Unit	Reference
λ	0.0006	1/year	[26]	Π	0.019	1/year	[26]
p_1	0.6	1/year	[26]	p_2	0.003264	1/year	fitted
p_3	0.012781	1/year	fitted	μ	0.012	1/year	fitted
ω	0.776507	1/year	fitted	β	0.55	1/year	[26]
$1-\theta$	0.831504	1/year	fitted	γ_1	0.186850	1/year	fitted
γ_2	0.000002	1/year	fitted	δ	0.055	1/year	[26]
α	0.2	1/year	[26]	σ	0.014326	1/year	fitted
ϵ	0.123033	1/year	fitted	τ	0.5	1/year	[26]
η	0.598350	1/year	fitted	–	–	–	–

Table 3. A summary of the facts, both actual and anticipated.

Statistics	Min	Q1	Q2 (Median)	Q3	Mean	Max	Standard Deviation
Real	164	3710	8350	10000	6780	11300	3930
Predicted	164	4160	8150	10100	6910	10900	3680

Table 4. Pertussis data in Austria, (ECDC dashboard [27]).

Year	Cases	C. cases
2022	164	164
2021	129	293
2020	632	925
2019	2233	3158
2018	2202	5360
2017	1411	6771
2016	1291	8062
2015	579	8641
2014	370	9011
2013	580	9591
2012	571	10162
2011	288	10450
2010	495	10945
2009	185	11070
2008	188	11258

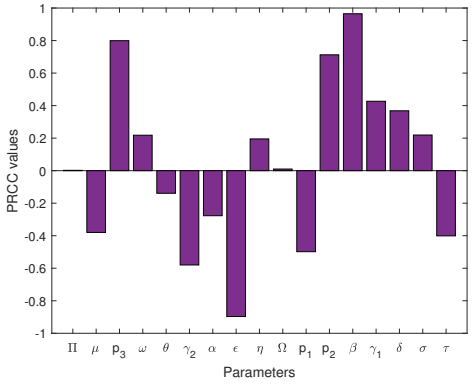

Figure 5. Figure showing the PRCC values of $\mathcal{R}_c$ versus the parameters of model (2).

life-time in the presence of controls, is obtained by putting S_u^0, S_v^0 and N^0,

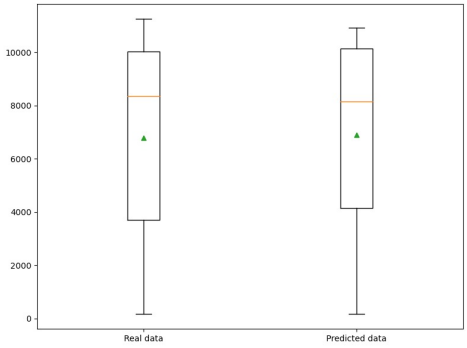

Figure 6. Box plotting to illustrate the effectiveness of awareness on infected individuals under treatment.

$$\mathcal{R}_c = \frac{\beta\mu\sigma(1-\epsilon)\left[(1-p_1)(k_2+(1-\theta)p_2)+p_1(\omega+(1-\theta)k_1)\right]\left[\eta(k_4\gamma_1+(1-\gamma_1)\gamma_2)+k_5(1-\gamma_1)\right]}{k_3k_4k_5\left[\mu k_2+p_2(\mu+p_3)\right]},$$

where $k_1 = \mu + p_2$, $k_2 = \omega + \mu + p_3$, $k_3 = \mu + \sigma$, $k_4 = \mu + \delta + \alpha + \gamma_2$ and $k_5 = \tau + \mu$.

The basic reproduction number can be calculated by setting all control parameters in (3.3) to zero, that is ($p_1 = p_2 = p_3 = \omega = \gamma_1 = \gamma_2 = \epsilon = \theta = 0$)

$$\mathcal{R}_0 = \frac{\beta\sigma\mu(\eta(1+\mu+\delta+\alpha)+\tau+\mu)}{\mu(\mu+\sigma)(\mu+\delta+\alpha)(\tau+\mu)} \tag{15}$$

3.4. Local stability of disease free equilibrium

theorem. For the model (2), the disease-free equilibrium (DFE) ϵ^0 is unstable if $mathcalR_c > 1$ and locally asymptotically stable (LAS) if $mathcalR_c < 1$ in Ω.

proof. A dynamical system is said to be locally asymptotically stable if small perturbations to the system do not cause significant changes in the trajectories of the system variables. Mathematically, local asymptotic stability can be established if the real parts of all eigenvalues of the Jacobian matrix, which represents the linearized system around the

Table 5. PRCC values for the parameters of model (2) using $\mathcal{R}_c$ as response functions, all the parameter values used are in Table. 3.

Parameter	PRCC values of $\mathcal{R}_c$	Parameter	PRCC values of $\mathcal{R}_c$
Π	0.0020	Ω	0.0100
μ	-0.3799	p_1	-0.4983
p_3	0.799225	p_2	0.7123
ω	0.2180	β	0.9649
$(1-\theta)$	-0.1391	γ_1	0.4268
γ_2	-0.5799	δ	0.3681
α	-0.2771	σ	0.2192
ϵ	-0.8969	τ	-0.4010
η	0.1952	-	-

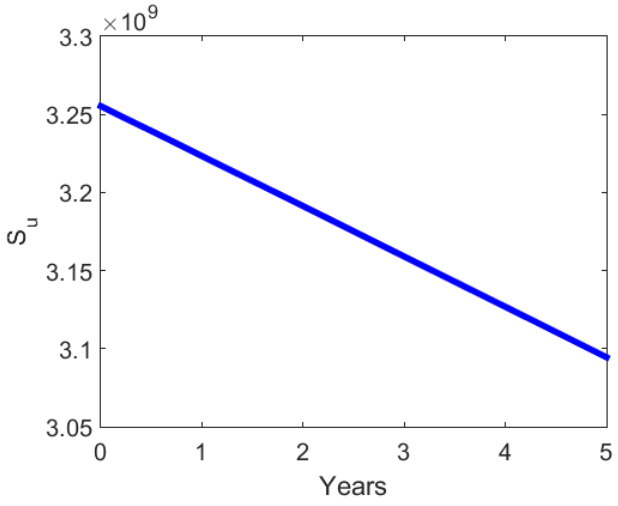

Figure 7. Behaviour of Susceptible un-vaccinated individuals.

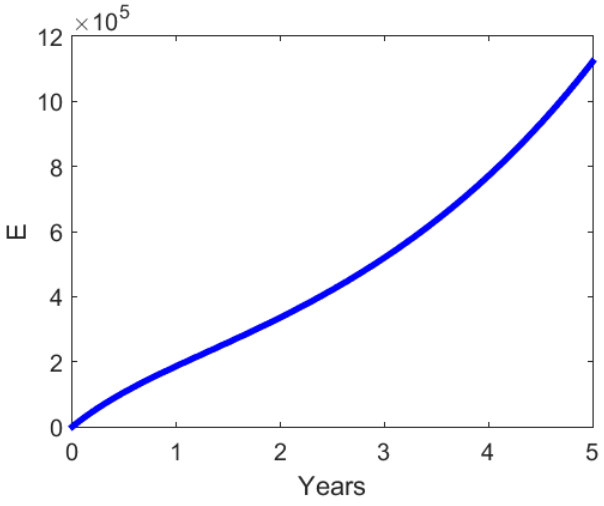

Figure 9. Behaviour of exposed individuals.

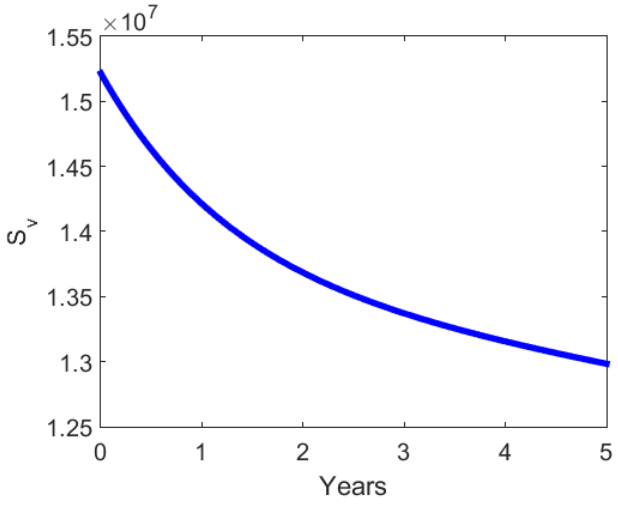

Figure 8. Behaviour of susceptible vaccinated individuals.

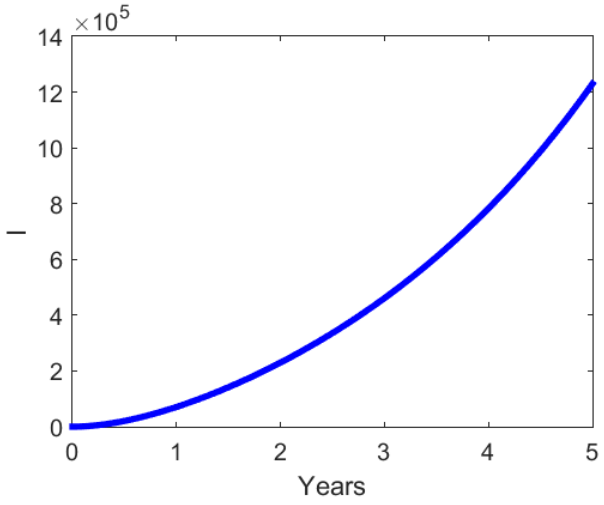

Figure 10. Behaviour of infectious individuals.

equilibrium point, are negative. The linearization of the system (2) at the disease-free equilibrium (DFE) yields the following linear system:

$$J(\epsilon^0)=\begin{bmatrix} -p_2-\mu & \omega & 0 & -\beta(1-\epsilon)N_1 & -\beta\eta(1-\epsilon)N_1 & 0 \\ P_2 & -k_2 & 0 & -\beta(1-\theta)(1-\epsilon)N_2 & -\beta(1-\theta)\eta(1-\epsilon)N_2 & 0 \\ 0 & 0 & -k_3 & \beta(1-\epsilon)(N_1+(1-\theta)N_2) & \beta\eta(1-\epsilon)(N_1+(1-\theta)N_2) & 0 \\ 0 & 0 & \sigma(1-\gamma_1) & -k_4 & 0 & 0 \\ 0 & 0 & \sigma\gamma_1 & \gamma_2 & -k_5 & 0 \\ 0 & p_3 & 0 & \alpha & \tau & -\mu \end{bmatrix} \quad (16)$$

where $N_1 = \frac{\mu((1-p_1)k_2+p_1\omega)}{k_1k_2-\omega p_2}, N_2 = \frac{\mu((1-p_1)p_2+k_1p_1)}{k_1k_2-\omega p_2}$.

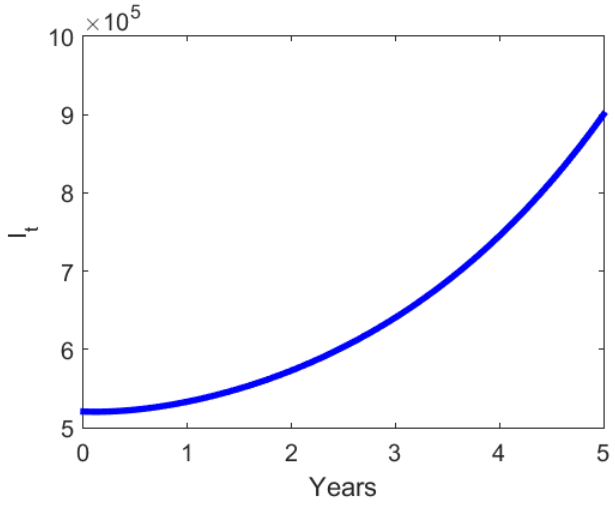

Figure 11. Behaviour of infectious individuals under treatment.

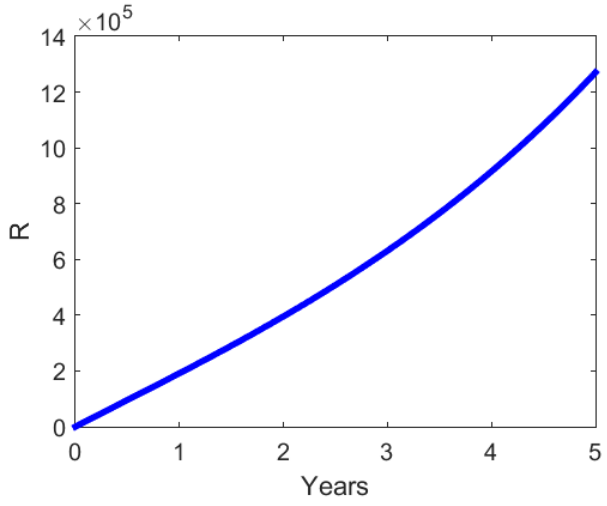

Figure 12. Behaviour of recovered individuals.

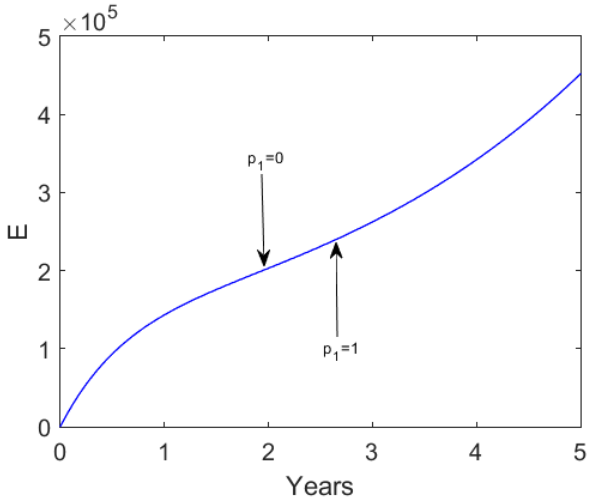

Figure 13. Impact of vaccination at recruitment on Exposed individuals.

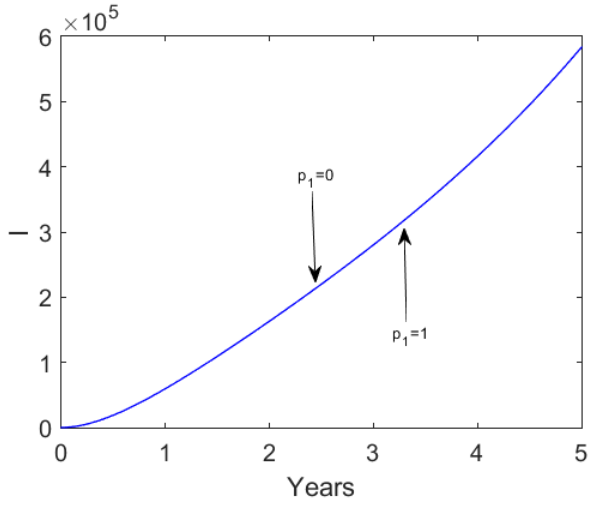

Figure 14. Impact of vaccination at recruitment on Infectious individuals.

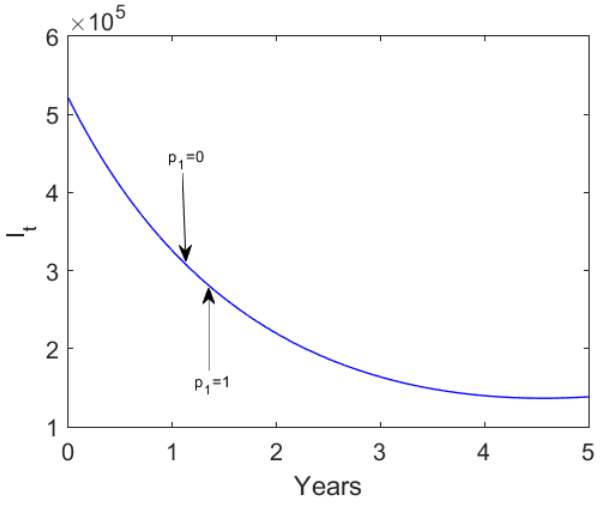

Figure 15. Impact of vaccination at recruitment on Infectious individuals under treatment.

Reducing (16) into row-echelon form we have (17) below,

$$\begin{bmatrix} m_{11} & m_{12} & 0 & m_{14} & m_{15} & 0 \\ 0 & \frac{m_{11}m_{22}-m_{12}m_{21}}{m_{11}} & 0 & \frac{m_{11}m_{24}-m_{14}m_{21}}{m_{11}} & \frac{m_{11}m_{25}-m_{15}m_{21}}{m_{11}} & 0 \\ 0 & 0 & m_{33} & m_{34} & m_{35} & 0 \\ 0 & 0 & 0 & \frac{m_{33}m_{44}-m_{34}m_{43}}{m_{33}} & -\frac{m_{43}m_{35}}{m_{33}} & 0 \\ 0 & 0 & 0 & 0 & \frac{m_{33}m_{44}m_{55}-m_{34}m_{43}m_{55}+m_{35}m_{43}m_{54}-m_{35}m_{44}m_{53}}{m_{33}m_{44}-m_{34}m_{43}} & 0 \\ 0 & 0 & 0 & 0 & 0 & m_{66} \end{bmatrix} \quad (17)$$

where

$$\begin{aligned} &m_{11} = -(p_2+\mu), \quad m_{12} = \omega, \quad m_{14} = -\beta(1-\epsilon)N_1, \quad m_{15} = -\beta\eta(1-\epsilon)N_1, \\ &m_{21} = p_2, \quad m_{22} = -k_2, \quad m_{24} = -\beta(1-\theta)(1-\epsilon)N_2, \quad m_{25} = -\beta(1-\theta)\eta(1-\epsilon), \\ &m_{33} = -k_3, \quad m_{34} = \beta(1-\epsilon)N_1 + \beta(1-\theta)(1-\epsilon)N_2, \\ &m_{35} = \beta\eta(1-\epsilon)N_1 + \beta(1-\theta)\eta(1-\epsilon)N_2, \quad m_{43} = \sigma(1-\gamma_1), \\ &m_{44} = -k_4, \quad m_{53} = \sigma\gamma_1, \quad m_{54} = \gamma_2, \quad m_{55} = -k_5, \\ &m_{62} = p_3, \quad m_{64} = \alpha, \quad m_{65} = \tau, \quad m_{66} = -\mu. \end{aligned} \quad (18)$$

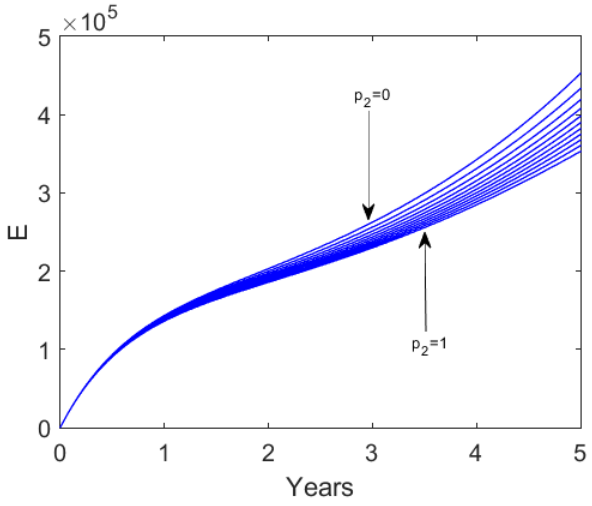

Figure 16. Impact of vaccination due to awareness on exposed individuals.

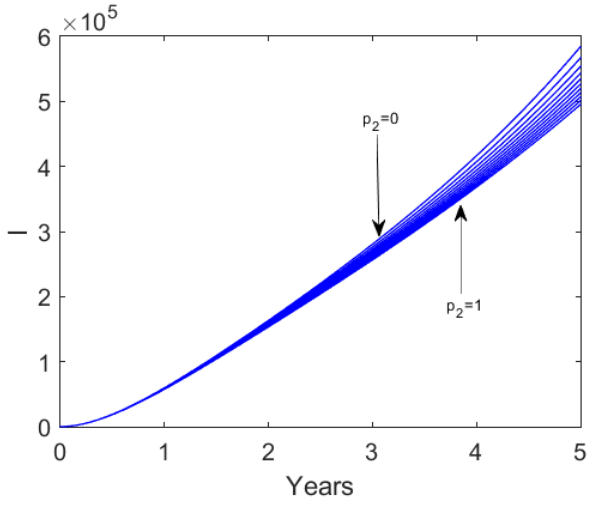

Figure 17. Impact of vaccination due to awareness on infectious individuals.

The eigenvalues of the system were computed using the mathematical software Maple, as shown below:

$$\begin{bmatrix} \lambda_1 = m_{66} \\ \lambda_2 = m_{33} \\ \lambda_3 = \frac{m_{33}\,m_{44} - m_{34}\,m_{43}}{m_{33}} \\ \lambda_4 = \frac{m_{33}\,m_{44}\,m_{55} - m_{34}\,m_{43}\,m_{55} + m_{35}\,m_{43}\,m_{54} - m_{35}\,m_{44}\,m_{53}}{m_{33}\,m_{44} - m_{34}\,m_{43}} \\ \lambda_5 = m_{11} \\ \lambda_6 = \frac{m_{11}\,m_{22} - m_{12}\,m_{21}}{m_{11}} \end{bmatrix}. \tag{19}$$

Clearly, λ_1, λ_2 and λ_5 are all negatives of (18). Now for the remaining eigenvalues we have,
For λ_3, after all simplification, we have

$$\lambda_3 = -\frac{k_3k_4 + \beta\mu\sigma(1-\epsilon)(1+\gamma_1)((1-p_1)k_2 + \omega p_2))}{k_3(\mu(\omega+\mu) + \mu(p_2p_3) + p_2p_3)}. \tag{20}$$

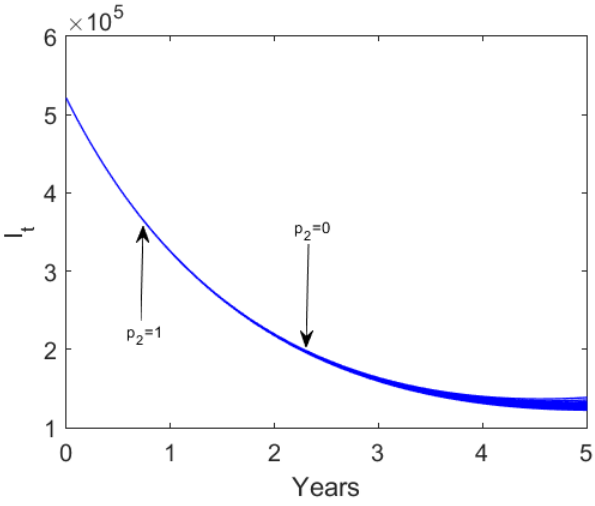

Figure 18. Impact of vaccination due to awareness on infectious individuals under treatment.

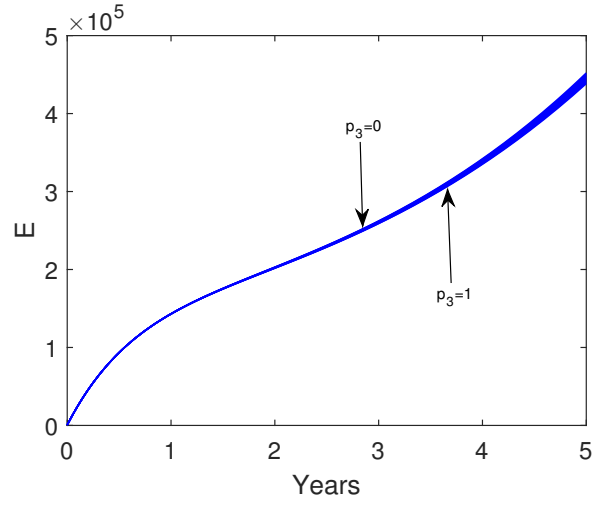

Figure 19. Impact of vaccination booster on exposed individuals.

For λ_4, after simplification we have

$$\frac{-k_3k_4k_5 + \beta\sigma(1-\epsilon)(N_1+(1-\theta)N_2)\left[(1-\gamma_1)k_5 + \eta(k_4\gamma_1 - (1-\gamma_1)\gamma_2 + (1-\gamma_1)k_5)\right]}{k_3k_4 - \beta\sigma(1-\epsilon)(N_1+(1-\theta)N_2)(1-\gamma_1)} < 0 \tag{21}$$

$$-k_3k_4k_5 + \beta\sigma(1-\epsilon)(N_1+(1-\theta)N_2)((1-\gamma_1)k_5 + \eta(k_4\gamma_1 - (1-\gamma_1)\gamma_2 + (1-\gamma_1)k_5) < 0, \tag{22}$$

if and only if

$$\beta\sigma(1-\epsilon)(N_1+(1-\theta)N_2)\left[(1-\gamma_1)k_5 + \eta(k_4\gamma_1 - (1-\gamma_1)\gamma_2 + (1-\gamma_1)k_5)\right] < k_3k_4k_5 \tag{23}$$

Putting N_1 and N_2 in (23) we have $\lambda_4 < 0$ if and only if

$$\frac{\beta\mu\sigma(1-\epsilon)\left[(1-p_1)k_2+(1-\theta)p_2\right]+p_2\left[\omega+(1-\theta)k_1\right]\left[(1-\gamma_1)k_5+\eta(k_4\gamma_1-(1-\gamma_1)\gamma_2+(1-\gamma_1)k_5)\right]}{k_3k_4k_5\left[\mu k_2+p_2(\mu+p_3)\right]} < 1 \tag{24}$$

The left-hand side of equation (24) corresponds to the control reproduction number $\mathcal{R}_c$ of equation (3.3). This means that the eigenvalue λ_5 is negative if and only if $\mathcal{R}_c$ is less than 1.
Lastly for λ_6 after simplification we have

$$\lambda_6 = -\frac{[\mu k_2 + p_2(\mu + p_3)]}{p_2 + \mu}. \tag{25}$$

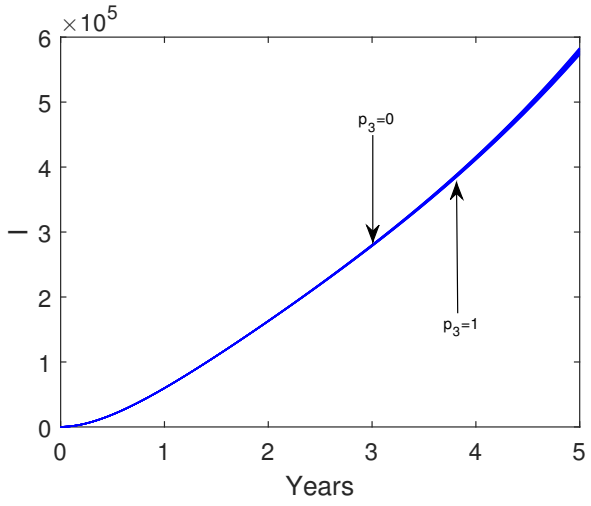

Figure 20. Impact of vaccination booster on infectious individuals.

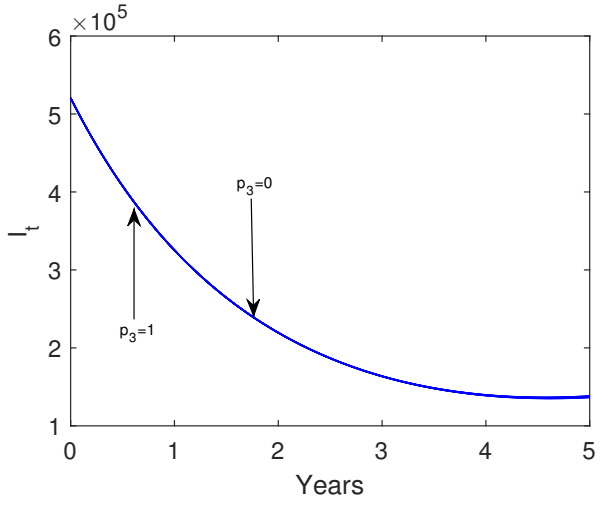

Figure 21. Impact of vaccination booster on infectious individuals.

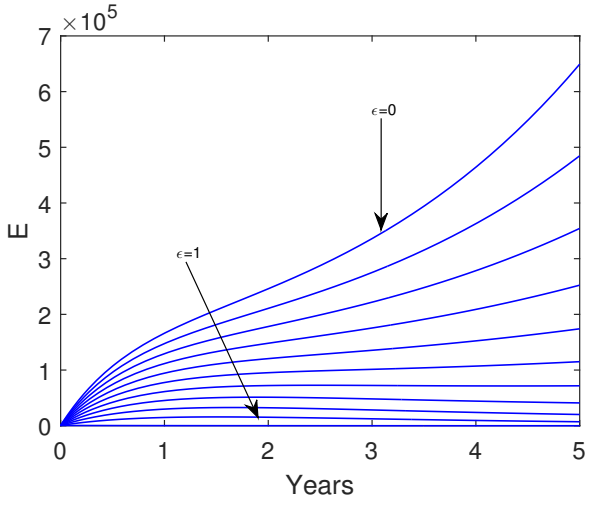

Figure 22. Impact of awareness on exposed individuals.

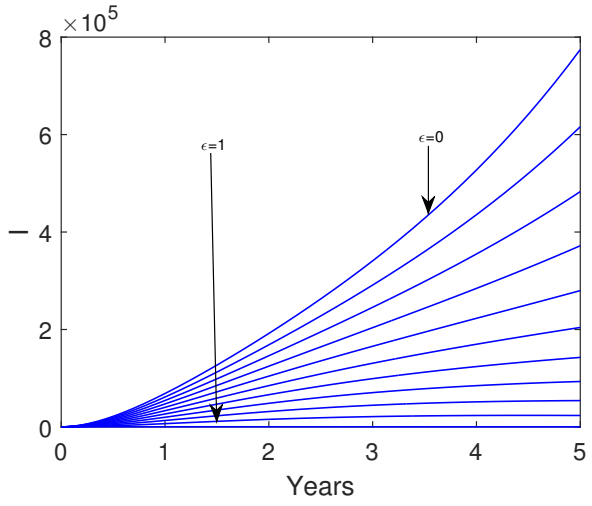

Figure 23. Impact of awareness on infectious individuals.

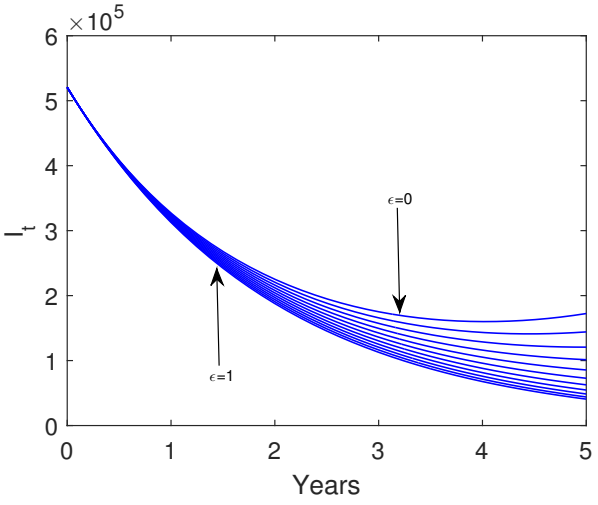

Figure 24. Impact of awareness on infectious individuals under treatment.

The results of the eigenvalue analysis show that when $\mathcal{R}_c < 1$, all the eigenvalues of the Jacobian matrix are negative, indicating that the disease-free equilibrium is locally asymptotically stable and otherwise unstable. This implies that small perturbations of the system do not significantly affect the dynamics of the system and that the disease will eventually disappear. Therefore, the theorem (3.4) is proven.

3.5. Global stability of disease-free equilibrium

theorem. For the model (2), the disease-free equilibrium (DFE) ϵ^0 is globally asymptotically stable (GAS) in Ω if $mathcalR_c < 1$, and unstable if $mathcalR_c > 1$.

proof.

$$\begin{aligned} \frac{dX_1}{dt} &= F(X_1, X_2), \\ \frac{dX_2}{dt} &= G(X_1, X_2); G(X_1, 0) = 0, \end{aligned} \tag{26}$$

where $X_1 = (S_u^0, S_v^0, R^0)$ and $X_2 = (E^0, I^0, I_t^0)$, where $X_1 \in R_+^3$ is denoting the uninfected population and $X_2 \in R_+^3$ denoting the infected pop-

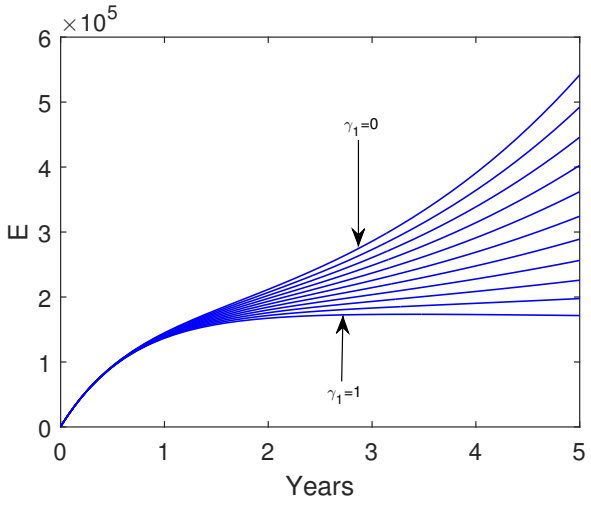

Figure 25. Impact of treatment due to awareness of the exposed individuals on exposed individuals.

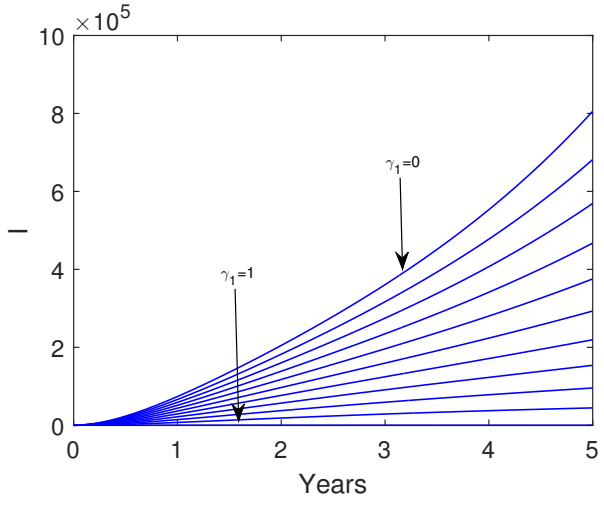

Figure 26. Impact of treatment due to awareness of the exposed individuals on infectious individuals.

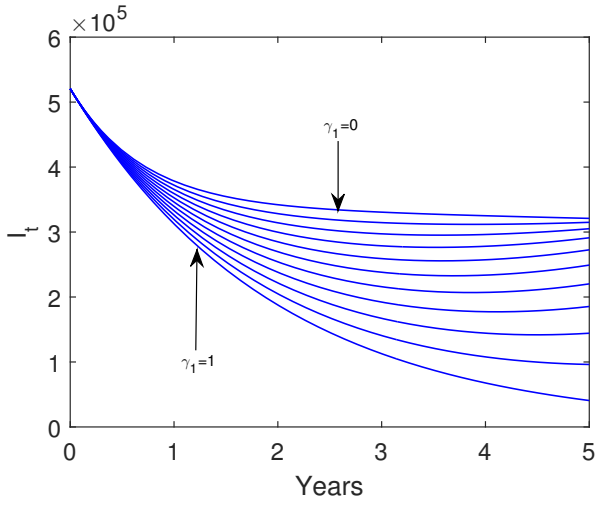

Figure 27. Impact of treatment due to awareness of the exposed individuals on infectious individuals under treatment.

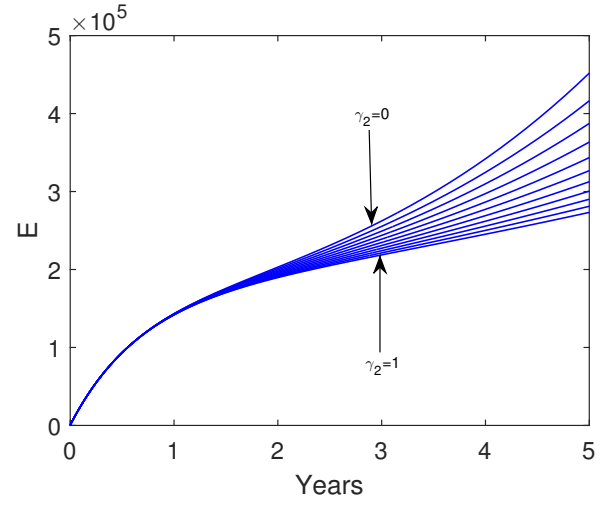

Figure 28. Impact of treatment due to awareness of the infectious individuals on exposed individuals.

ulation. The disease-free equilibrium is now denoted as, $M^0 = (X_1^*, 0)$, where $X_1^* = (N^0, 0)$.
Now for the first condition, globally asymptotic stability of X_1^*, gives

$$\frac{dX_1}{dt} = F(X_1, 0) = \begin{bmatrix} \Pi(1-p_1) + \omega S_v - (p_2+\mu)S_u^0 \\ \Pi p_1 + p_2 S_u - (\omega+\mu+p_3)S_v^0 \\ p_3 S_v - \mu R^0 \end{bmatrix}. \tag{27}$$

A linear ODE solving gives the following.

$$\begin{aligned} &\frac{\Pi(1-p_1)+\omega S_v}{(p_2+\mu)} - \frac{\Pi(1-p_1)}{(p_2+\mu)} e^{-(p_2+\mu)t} \\ &+ S_u^0(0)e^{-(p_2+\mu)t} = S_u^0(t), \\ &\frac{\Pi p_1 + p_2 S_u^0}{(\omega+\mu+p_3)} - \frac{\Pi p_1 + p_2 S_u^0}{\omega+\mu+p_3} e^{-(\omega+\mu+p_3)t} \\ &+ S_v^0(0)e^{-(\omega+\mu+p_3)t} = S_v^0(t), \\ &\frac{p_3 S_v^0}{\mu} - \frac{p_3 S_v^0}{\mu} e^{-\mu t} + R^0(0)e^{-\mu t} = R^0(t). \end{aligned} \tag{28}$$

Now, clearly from system (2) we have $S_u^0(t)+S_v^0(t)+R^0(t) \to N^0(t)$ as $t \to \infty$ regardless of the value of $S_u^0(t), S_v^0(t)$ and $R^0(t)$. Thus , $X_1^* = (N^0, 0)$ is globally asymptotically stable.
Next, for the second condition, that is $\tilde{G}(X_1, X_2) = AX_2 - G(X_1, X_2) \geq 0$

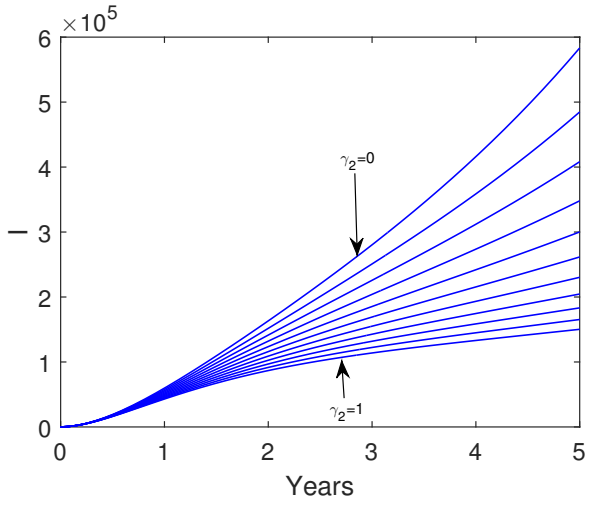

Figure 29. Impact of treatment due to awareness of the infectious individuals on infectious individuals.

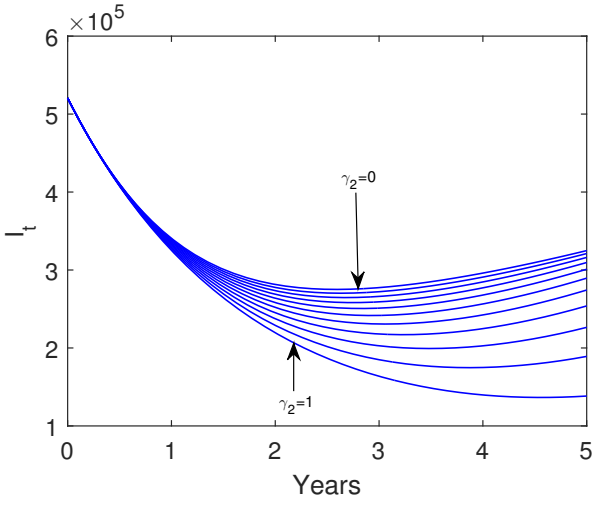

Figure 30. Impact of treatment due to awareness of the infectious individuals on infectious individuals under treatment.

$$A = \begin{pmatrix} -k_3 & \Psi_1 & \Psi_2 \\ \sigma(1-\gamma_1) & -k_4 & 0 \\ \sigma\gamma_1 & \gamma_2 & -k_5 \end{pmatrix}, \tag{29}$$

where

$$\Psi_1 = \frac{\beta(1-\epsilon)(S_u + (1-\theta)S_v)}{N}$$
$$\Psi_2 = \frac{\beta\eta(1-\epsilon)(S_u + (1-\theta)S_v)}{N}. \tag{30}$$

The matrix A is a Metziller matrix (the non-diagonal elements of are non-negative).

$$G(X_1, X_2) = \begin{pmatrix} \frac{(1-\epsilon)\beta(I+\eta I_t)}{N} S_u + \frac{(1-\epsilon)(1-\theta)\beta(I+\eta I_t)}{N} S_v - k_3 E \\ \sigma(1-\gamma_1)E - k_4 I \\ \sigma\gamma_1 E + \gamma_2 I - k_5 I_t \end{pmatrix}, \tag{31}$$

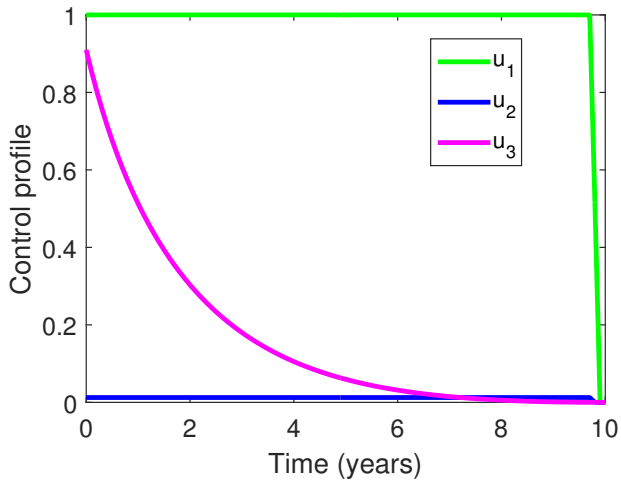

Figure 31. Figure showing the control profile of model (46).

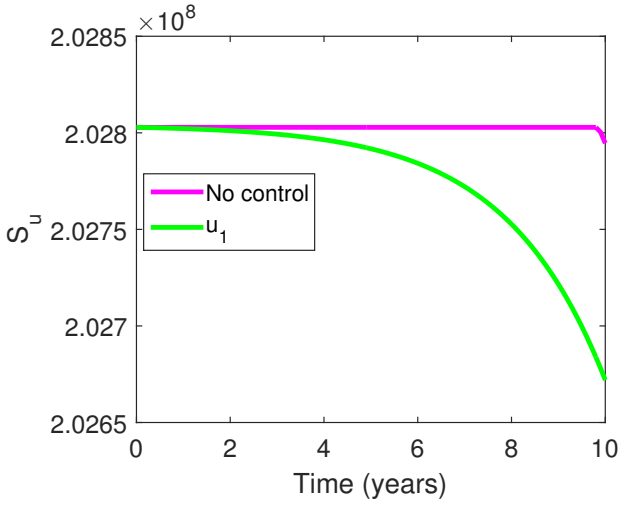

Figure 32. Influence of health education control on un-vaccinated susceptible individuals.

then

$$\tilde{G}(X_1, X_2) = AX_2 - G(X_1, X_2) = \begin{bmatrix} 0 \\ 0 \\ 0 \end{bmatrix},$$

that is

$$\tilde{G}(X_1, X_2) = \begin{bmatrix} 0 & 0 & 0 \end{bmatrix}^T.$$

It is obvious that $\tilde{G}(X_1, X_2) = 0$.

3.6. Existance of equilibria

At every equilibrium state, let $S_u(t)$, $S_v(t)$, $E(t)$, $I(t)$, $I_t(t)$, and $R(t)$ represent the solutions of system (2). We compare the rate of change with zero at equilibrium. In other words, setting all the equations in the system (2) to zero, we can use the Maple program to get the equi-

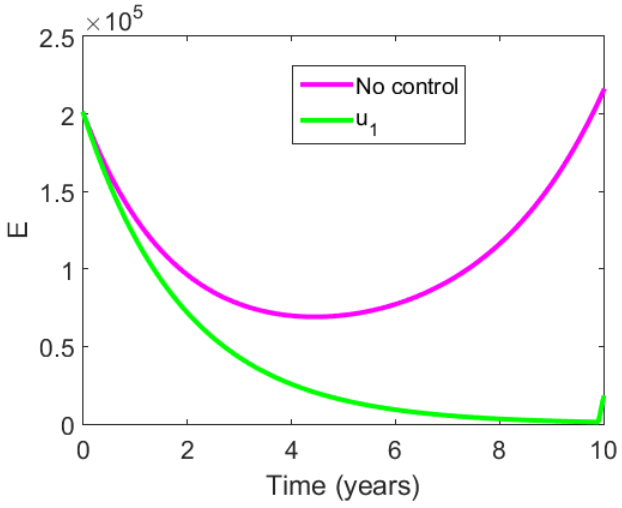

Figure 33. Impact of treatment due to awareness of the exposed individuals.

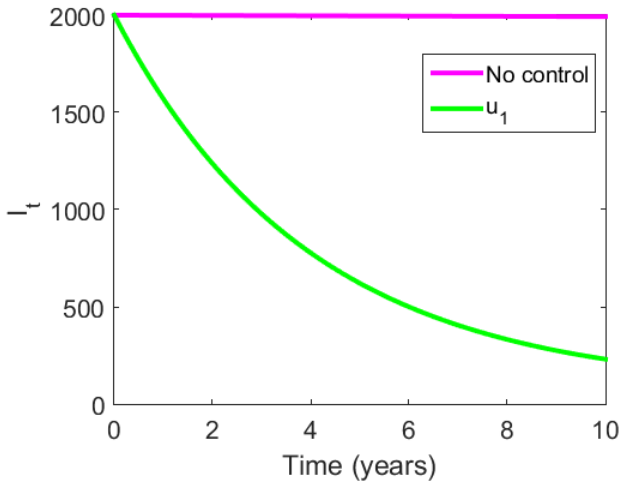

Figure 35. Influence of health education control on infected under treatment individuals.

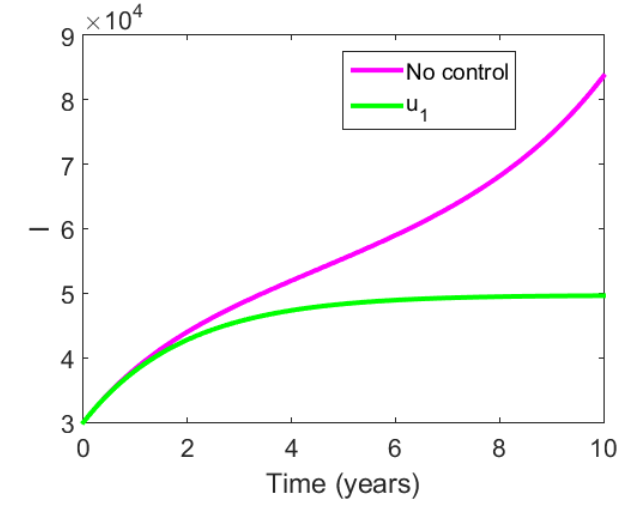

Figure 34. Influence of health education control on infected individuals.

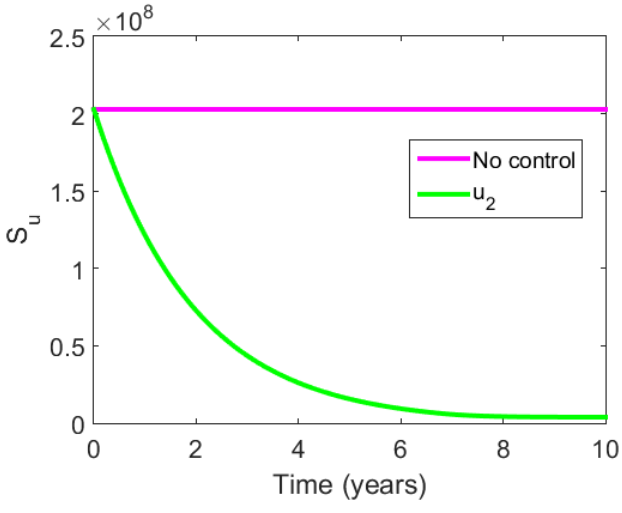

Figure 36. Influence of vaccination control on un-vaccinated susceptible individuals.

librium solutions, which look like this;

$$
\begin{aligned}
S_u^* &= \frac{\Pi\left((1-\theta)\lambda^*(1-p_1)+(1-p_1)k_2+\omega p_1\right)}{(1-\theta)\lambda^*(\lambda+k_1)+\lambda^* k_2-\omega p_2+k_1k_2},\\
S_v^* &= \frac{\Pi\left((1-p_1)p_2+(\lambda+k_1)p_1\right)}{(1-\theta)\lambda^*(\lambda+k_1)+\lambda^* k_2-\omega p_2+k_1k_2},\\
E^* &= \frac{\lambda\Pi\left((1-p_1)k_2+(1-p_1)(1-\theta)p_2+(\lambda+k_1)(1-\theta)+\omega p_1\right)}{k_3\left((1-\theta)\lambda^*+\lambda^* k_2-\omega p_2+k_1k_2\right)},\\
I^* &= \frac{\lambda\Pi\sigma(1-\gamma_1)\left((1-p_1)k_2+(1-p_1)(1-\theta)p_2+(\lambda+k_1)(1-\theta)+\omega p_1\right)}{k_3k_4\left((1-\theta)\lambda^*+\lambda^* k_2-\omega p_2+k_1k_2\right)},\\
I_t^* &= \frac{\lambda\Pi\sigma(1-\gamma_1)\left((1-p_1)k_2+(1-p_1)(1-\theta)p_2+(\lambda+k_1)(1-\theta)+\omega p_1\right)}{k_3k_4k_5\left((1-\theta)\lambda^*+\lambda^* k_2-\omega p_2+k_1k_2\right)},\\
R^* &= \frac{p_3\Pi\left((1-p_1)p_2+(\lambda+k_1)p_1\right)}{\mu\left((1-\theta)\lambda^*(\lambda+k_1)+\lambda^* k_2-\omega p_2+k_1k_2\right)}\\
&+\frac{\lambda\Pi\sigma\alpha(1-\gamma_1)\left((1-p_1)k_2+(1-p_1)(1-\theta)p_2+(\lambda+k_1)(1-\theta)+\omega p_1\right)}{\mu k_3k_4\left((1-\theta)\lambda^*+\lambda^* k_2-\omega p_2+k_1k_2\right)}\\
&+\frac{\lambda\Pi\tau\sigma(1-\gamma_1)\left((1-p_1)k_2+(1-p_1)(1-\theta)p_2+(\lambda+k_1)(1-\theta)+\omega p_1\right)}{\mu k_3k_4k_5\left((1-\theta)\lambda^*+\lambda^* k_2-\omega p_2+k_1k_2\right)}.
\end{aligned}
\tag{32}
$$

3.7. Existence of endemic equilibrium

To determine the existence of an endemic Equilibrium, Descartes' rule of signs is used. Now in the endemic state, the force of infection is given by

$$\lambda^* = \beta(1-\epsilon)\left(\frac{I^*+\eta I_t^*}{N^*}\right), \tag{33}$$

where,

$$N^* = S_u^* + S_v^* + E^* + I^* + I_t^* + R^*.$$

Substituting for the endemic equilibrium points into the force of infection above gives $\lambda^* = 0$. equivalent to DFE, which is stable, and the following quadratic equation in terms of λ^*,

$$B_1\lambda^2 + B_2\lambda + B_3 = 0, \tag{34}$$

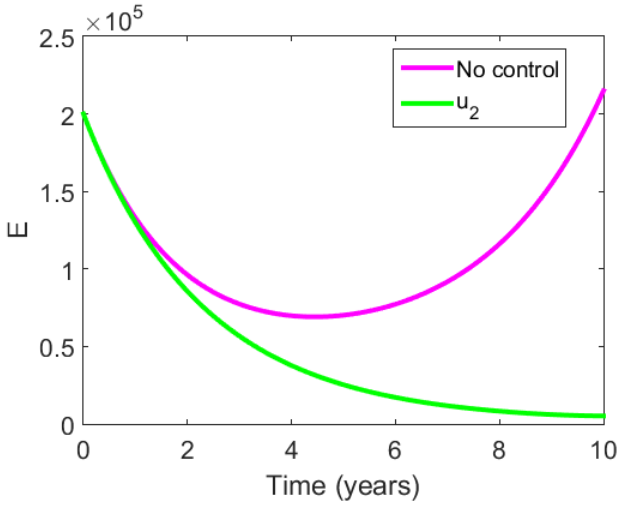

Figure 37. Influence of vaccination control on exposed individuals.

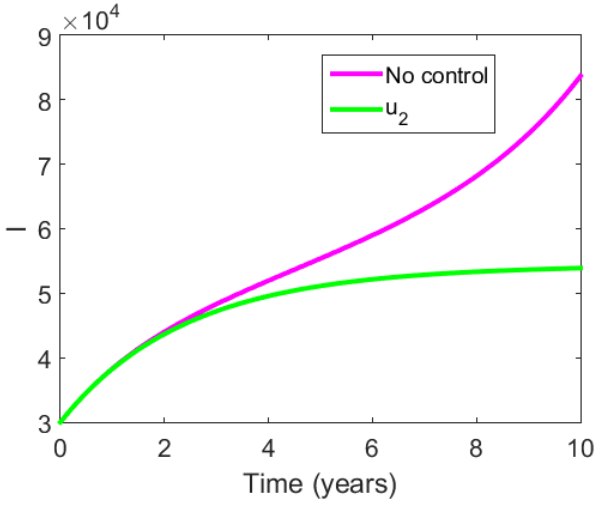

Figure 38. Influence of vaccination control on infected individuals.

where

$$
\begin{aligned}
B_1 &= k_4k_5(1-\theta)\Pi + (1-\theta)\Pi\sigma(1-\gamma_1)(k_5+1)\\
&\quad + k_5\Pi\alpha\sigma(1-\gamma_1)(1-\theta) + \Pi\tau\sigma(1-\gamma_1)(1-\theta)\\
B_2 &= k_3k_4k_5(1-\theta)(1-p_1)\Pi + k_3k_4k_5p_1\Pi + k_4k_5\Pi(1-p_1)p_2\\
&\quad + k_4k_5\Pi(1-p_1)(1-\theta)p_2 + k_4k_5\Pi\left((1-\theta)k_1+\omega p_1\right)\\
&\quad + k_5\Pi\sigma(1-\gamma_1)(1-p_1)k_2 + k_5\Pi\sigma(1-\gamma_1)(1-p_1)(1-\theta)p_2\\
&\quad + \Pi\sigma(1-\gamma_1)k_5\left((1-\theta)k_1+\omega p_1\right)\\
&\quad + \Pi\sigma(1-\gamma_1)(1-p_1)k_2 + \Pi\sigma(1-\gamma_1)(1-p_1)(1-\theta)p_2\\
&\quad + \Pi\sigma(1-\gamma_1)\left((1-\theta)k_1+\omega p_1\right) + k_3k_4k_5\Pi p_1p_3\\
&\quad + \Pi\sigma\alpha(1-\gamma_1)k_5(1-p_1)k_2 + \Pi\sigma\alpha(1-\gamma_1)k_5(1-p_1)(1-\theta)p_2\\
&\quad + (1-\theta)k_1 + \omega p_1 + \Pi\sigma\tau(1-\gamma_1)k_5(1-p_1)k_2\\
&\quad + \Pi\sigma\tau(1-\gamma_1)k_5(1-p_1)(1-\theta)p_2\\
&\quad + \Pi\sigma\tau(1-\gamma_1)k_5(1-\theta)k_1 + \omega p_1\\
&\quad - (1-\epsilon)\beta\Pi\sigma(1-\gamma_1)k_5(1-\theta)\\
&\quad - (1-\epsilon)\beta\Pi\sigma\eta(1-\gamma_1)(1-\theta)\\
B_3 &= \Pi k_3k_4k_5[\mu k_2 + p_2(\mu+p_3)](1-\mathcal{R}_c)
\end{aligned}
\tag{35}
$$

theorem. The system (2) has:

- no endemic equilibrium if $B_2 > 0 \Longleftrightarrow \mathcal{R}_c < 1$
- a unique endemic equilibrium if $B_2 < 0 \Longleftrightarrow \mathcal{R}_c > 1$

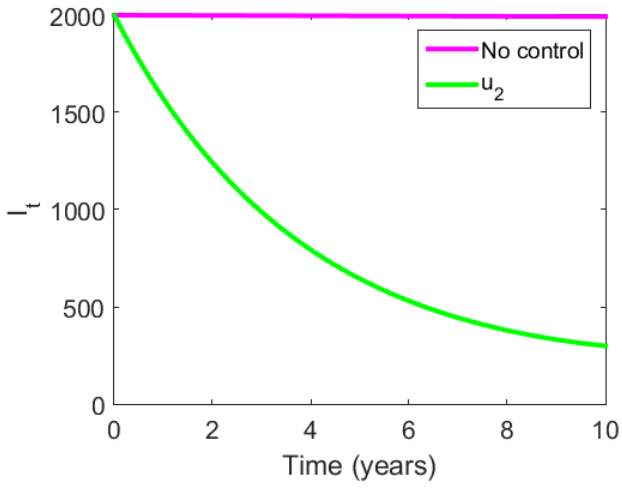

Figure 39. Influence of vaccination control on infected individuals under treatment.

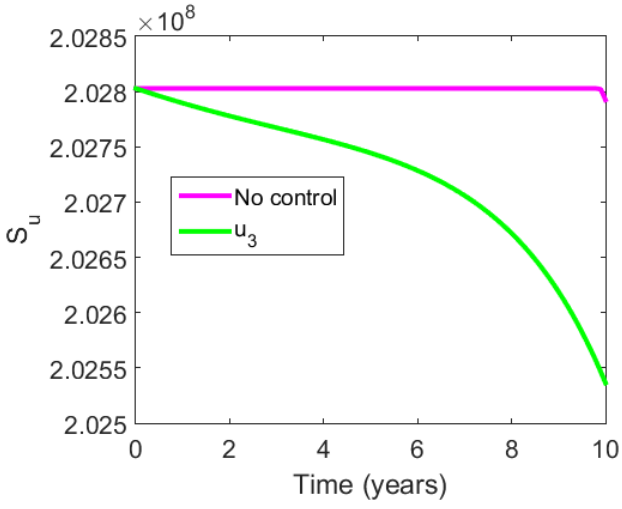

Figure 40. Influence of treatment control on un-vaccinated susceptible individuals.

- a unique endemic equilibrium if $B_2 > 0 \Longleftrightarrow \mathcal{R}_c > 1$
- two positive equilibrium if $B_2 < 0 \Longleftrightarrow \mathcal{R}_c < 1$ and $B_2^2 - 4B_1B_3 > 0$.

3.8. Global Asymptotic Stability (GAS) of Pertussis Equilibrium Endemic Point (PEEP)

Let

$$\mathcal{D}^{**} = \{(S_u^{**}, S_v^{**}, E^{**}, I^{**}, I_t^{**}, R^{**}) \in \mathcal{E}^{**}\} \tag{36}$$

be a stable manifold of $\mathcal{E}^{**}$.

Theorem. The PEEP of model (2) is GAS in $\mathcal{D}^{**}$ with the conditions that $\omega = P_2 = \gamma_1 = \delta = P_3 = \alpha = 0$ whenever $\mathcal{R}_c > 1$.

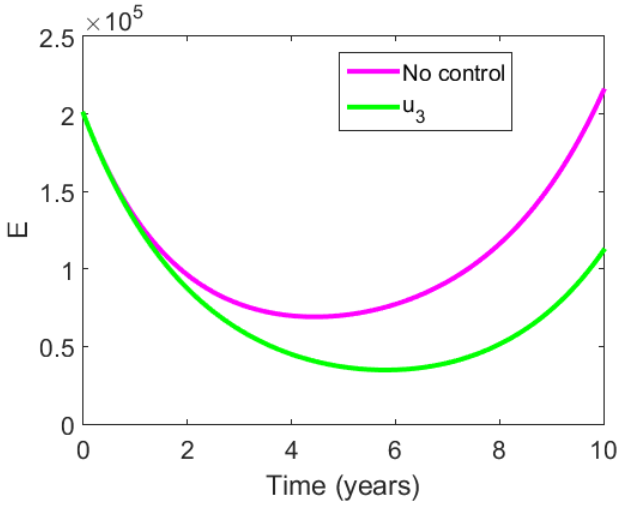

Figure 41. Influence of treatment control on exposed individuals.

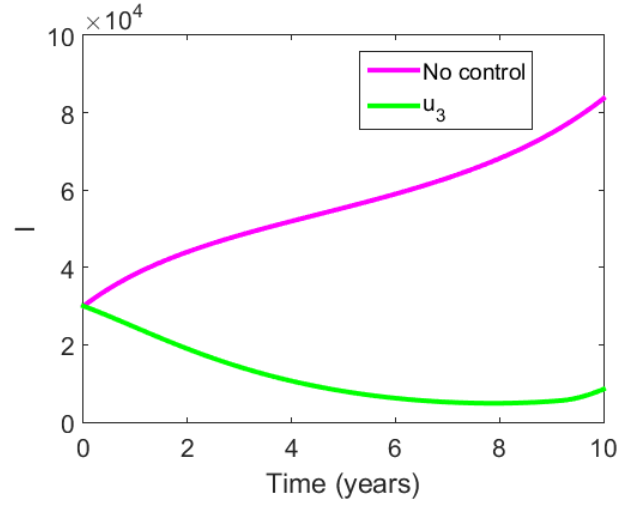

Figure 42. Influence of treatment control on infected individuals.

Proof. Let $\mathcal{F}$ be a Goh-Volterra type of Lyapunov function, as given below

$$\begin{aligned}\mathcal{F} &= \left(S_u - S_u^{**} - S_u^{**} ln\frac{S_u}{S_u^{**}}\right)\\ &+ \left(S_v - S_v^{**} - S_v^{**} ln\frac{S_v}{S_v^{**}}\right)\\ &+ \left(E - E^{**} - E^{**} ln\frac{E}{E^{**}}\right)\\ &+ \frac{k_1^*}{\sigma}\left(I - I^{**} - I^{**} ln\frac{I}{I^{**}}\right)\\ &+ \frac{k_1^* k_2^*}{\sigma\gamma_2}\left(I_t - I_t^{**} - I_t^{**} ln\frac{I_t}{I_t^{**}}\right)\\ &+ \frac{k_1^* k_2^* k_3^*}{\sigma\gamma_2\tau}\left(R - R^{**} - R^{**} ln\frac{R}{R^{**}}\right),\end{aligned} \tag{37}$$

where

$$k_1^* = \mu + \sigma, k_2^* = \mu + \gamma_2, k_3^* = \mu + \tau$$

, differentiating equation (37) with respect to time, we have

$$\begin{aligned}\dot{\mathcal{F}} &= \left(1 - \frac{S_u^{**}}{S_u}\right)\dot{S_u} + \left(1 - \frac{S_v^{**}}{S_v}\right)\dot{S_v}\\ &+ \left(1 - \frac{E^{**}}{E}\right)\dot{E} + \frac{k_1^*}{\sigma}\left(1 - \frac{I_1^{**}}{I_1}\right)\dot{I_1}\\ &+ \frac{k_1^* k_2^*}{\sigma\gamma_2}\left(1 - \frac{I_2^{**}}{I_2}\right)\dot{I_2} + \frac{k_1^* k_2^* k_3^*}{\sigma\gamma_2\tau}\left(1 - \frac{R^{**}}{R}\right)\dot{R},\end{aligned} \tag{38}$$

substituting equation (2) into (38), we have

$$\begin{aligned}\dot{\mathcal{F}} &= \left(1 - \frac{S_h^{**}}{S_h}\right)(\Pi(1-p_1) - \lambda S_u - \mu S_u)\\ &+ \left(1 - \frac{S_v^{**}}{S_v}\right)(\Pi p_1 - (1-\theta)\lambda S_v - \mu S_v)\\ &+ \left(1 - \frac{E^{**}}{E}\right)(\lambda S_u + (1-\theta)\lambda S_v - k_1 E)\\ &+ \frac{k_1^*}{\sigma}\left(1 - \frac{I_1^{**}}{I_1}\right)(\sigma E - k_2 I)\\ &+ \frac{k_1^* k_2^*}{\sigma\gamma_2}\left(1 - \frac{I_2^{**}}{I_2}\right)(\gamma_2 I - k_3 I_t)\\ &+ \frac{k_1^* k_2^* k_3^*}{\sigma\gamma_2\tau}\left(1 - \frac{R^{**}}{R}\right)(\tau I_t - \mu R)\end{aligned} \tag{39}$$

with relations

$$\begin{aligned}\Pi(1-p_1) &= \lambda^{**} S_u^{**} + \mu S_u^{**},\\ \Pi p_1 &= (1-\theta)\lambda S_v^{**} + \mu S_v^{**}\end{aligned} \tag{40}$$

$$\begin{aligned}k_1^* E** &= \lambda^{**} S_u^{**} + (1-\theta)\lambda S_v^{**},\\ k_2^* I^{**} &= \sigma^{**} E^{**},\\ k_3^* I_t^{**} &= \gamma_2 I^{**},\\ \mu R^{**} &= \tau I_t^{**},\end{aligned}$$

by substituting first two equations in (40), equation (39) becomes

$$\begin{aligned}\dot{\mathcal{F}} &= \left(1 - \frac{S_u^{**}}{S_u}\right)(\lambda^{**} S_u^{**} + \mu S_u^{**} - \lambda S_u - \mu S_u)\\ &+ \left(1 - \frac{S_v^{**}}{S_v}\right)((1-\theta)\lambda S_v^{**} + \mu S_v^{**})\\ &+ \left(1 - \frac{S_v^{**}}{S_v}\right)(-(1-\theta)\lambda S_v - \mu S_v)\\ &+ \left(1 - \frac{E^{**}}{E}\right)(\lambda S_u + (1-\theta)\lambda S_v - k_1 E)\\ &+ \frac{k_1^*}{\sigma}\left(1 - \frac{I_1^{**}}{I_1}\right)(\sigma E - k_2 I)\\ &+ \frac{k_1^* k_2^*}{\sigma\gamma_2}\left(1 - \frac{I_2^{**}}{I_2}\right)(\gamma_2 I - k_3 I_t)\\ &+ \frac{k_1^* k_2^* k_3^*}{\sigma\gamma_2\tau}\left(1 - \frac{R^{**}}{R}\right)(\tau I_t - \mu R).\end{aligned} \tag{41}$$

Substituting third to sixth equations in equation (40), equation (41) and simplify, becomes

$$\begin{aligned}\dot{\mathcal{F}} &\le \mu S_u^{**}\left(2 - \frac{S_u}{S_u^{**}} - \frac{S_u^{**}}{S_u}\right) + \mu S_v^{**}\left(2 - \frac{S_v}{S_v^{**}} - \frac{S_v^{**}}{S_v}\right)\\ &+ \lambda^{**} S_u^{**}\left(6 - \frac{S_u^{**}}{S_u} - \frac{R}{R^{**}} - \frac{S_u E^{**}}{S_u^{**} E} - \frac{E I^{**}}{E^{**} I} - \frac{I I_t^{**}}{I^{**} I_t} - \frac{I_t R^{**}}{I_t^{**} R}\right)\\ &+ (1-\theta)\lambda^{**} S_v^{**}\left(6 - \frac{S_v^{**}}{S_v} - \frac{R}{R^{**}} - \frac{S_v E^{**}}{S_v^{**} E} - \frac{E I^{**}}{E^{**} I_1} - \frac{I I_t^{**}}{I^{**} I_t} - \frac{I_t R^{**}}{I_t^{**} R}\right),\end{aligned} \tag{42}$$

Using the relation of arithmetic mean to geometric mean, we then have

$$\left(2-\frac{S_u}{S_u^{**}}-\frac{S_u^{**}}{S_u}\right)\leq 0,\left(2-\frac{S_v}{S_v^{**}}-\frac{S_v^{**}}{S_v}\right)\leq 0,$$
$$\left(6-\frac{S_u^{**}}{S_u}-\frac{R}{R^{**}}-\frac{S_uE^{**}}{S_u^{**}E}-\frac{EI^{**}}{E^{**}I}-\frac{II_t^{**}}{I^{**}I_t}-\frac{I_tR^{**}}{I_t^{**}R}\right)\leq 0, \quad (43)$$
$$\left(6-\frac{S_v^{**}}{S_v}-\frac{R}{R^{**}}-\frac{S_vE^{**}}{S_v^{**}E}-\frac{EI^{**}}{E^{**}I_1}-\frac{II_t^{**}}{I^{**}I_t}-\frac{I_tR^{**}}{I_t^{**}R}\right)\leq 0.$$

Hence, we have $\dot{\mathcal{F}}\leq 0$ with conditions that $\omega=p_2=\gamma_1=\delta=p_3=\alpha=0$ and $\mathcal{R}_c>1$, since all the concerned variable in the model such as S_u, S_v, E, I, I_t and R are at steady state (pertussis endemic steady state), this can be substituted into the concerned variable of equation (2) to give

$$\lim_{t\to\infty}(S_u(t),S_v(t),E(t),I(t),I_t(t),R(t))\to(S_u^{**},S_v^{**},E^{**},I^{**},I_t^{**},R^{**}). \quad (44)$$

Hence, using Lassalle's invariant principle [28–34], the pertussis endemic equilibrium point is globally asymptotically stable (GAS).

4. Model fittings and parameter estimation

Determining accurate parameter values for mathematical models built with real-world data is a crucial but challenging step. This difficulty stems from the inherent inability to directly measure these parameters from the collected data. Therefore, estimation techniques are essential. The initial dynamics of the disease and relevant demographic factors can provide preliminary estimates of some parameters. The literature can also offer benchmark values. However, relying solely on literature can lead to incongruous results due to variations in data collection periods (days to years) and potential inaccuracies. Although there are numerous parameter estimation methods that exist, the least-squares method remains the most prevalent choice, despite the availability of alternatives. Even with validated models, parameter estimation remains a significant hurdle. To ensure that our proposed Pertussis model accurately reflects reality, we used parameter estimation using empirical data with realistic bounds. This approach yields parameter values specific to our model, avoiding dependence on values from other models.

We used patient data, as mentioned in Table 4, for the fitting of the least squares curve to estimate the parameters of the model. Data spanning 13 years (2008-2022) from the ECDC dashboard [27] was used to perform the least squares fit. The optimization process minimized the sum of squared errors (SSE) between the actual Pertussis data for severe cases and the predicted values of the model. Table 2 summarizes the estimated biological parameters and their corresponding values. Figure 2 visually demonstrates the agreement between the fitted curve (red line) and the actual data points (blue circles). It may also be noted that the value of R-squared is 0.987157, which is further evidence of the better agreement of the predicted values with those of the real data, while the basic reproduction number found using Eq. (3.3) is $\approx$ 1.29105. Figure 3 displays the residuals. Statistical summaries in Figure 4 indicate the absence of outliers, further supported by the summary table (Table 3).

The least squares method minimizes the residuals between the observed infection data ($\hat{y}_j$) and the simulated values obtained from the model equations, $g(t_j, y_j)$. Mathematically, this is represented by:

$$Residual=\frac{1}{N}\sum_{j=0}^{N}(\hat{y}_j-y_j)^2, \quad (45)$$

where:

- N = total number of data points
- $\hat{y}_j$ = observed infection data at time point j
- y_j = simulated infection data at time point j from the model.

This objective function was minimized using Python 3.12.1's built-in 'scipy' functions for solving ordinary differential equations (ODEs) and curve fitting. The initial conditions used for parameter estimation are provided as follows:

$$S_u(0)=3255221585, S_v(0)=15215578, E(0)=543, I(0)=164, I_t(0)=520580, R(0)=215.$$

4.1. Uncertainty and Sensitivity Analysis

In this section, the uncertainty and sensitivity analysis of all the parameters of the model (2) will be discussed. Most of the time, we usually see some parameters as potential parameters that can be used to control disease, but when their sensitivity on the reproduction number is tested, it proves otherwise, that is what we call uncertainty that surrounds the parameters of the model. Also, we usually see some parameters as potential parameters that cannot be used to control disease, but when their sensitivity on the reproduction number is tested, it proves otherwise, which is also an uncertainty that surrounds the parameters of the model.

Analyzing responsiveness and vulnerability is essential for investigating the behaviour of some complex models, as predicting the potential drawbacks of some information limits is fraught with risk due to the models' inherent complexity. In this section, the effects of each model boundary were assessed using the partial rank correlation coefficient (PRCC) and Latin Hypercube Sampling (LHS). The strongest and most intense factors that either raise or lower (transmission) the control parameter are found through sensitivity analysis. The most sensitive indicators of the spread of the disease are those that produce favourable outcomes for the number of infected individuals and successful reproduction; if these parameters increase or decrease, pertussis transmission will follow suit. The parameters that show negative values for the control reproduction number and the number of infected individuals are the most susceptible to stopping the spread; if these parameters increase, the rate of transmission of Pertussis will decrease.

5. Optimal control problem analysis

Finding the optimal control that minimizes or maximizes an objective functional that is dependent on the original purpose of adding the control to the model is the aim of optimal control optimization. Currently, reducing vulnerability among unvaccinated, exposed, and infected individuals through health education, vaccination, and treatment. Reducing the population of vulnerable people who are not vaccinated, exposed and infectious persons through three (3) controls, health education, vaccination, and treatment, is the goal of optimisation. The reformed model below identifies time-dependent controls, such as the influence of health education, vaccination, and treatment,

which are now functions of time. The model (2) remains unchanged.

$$\begin{aligned}
\frac{dS_u}{dt} &= \Pi(1-p_1) + \omega S v - (1-u_1(t))\lambda S_u \\
&\quad - (\mu + p_2)S_u, \\
\frac{dS_v}{dt} &= \Pi p_1 + p_2 S_u - (1-u_2(t))(1-\theta)\lambda S_v \\
&\quad - (\omega + \mu + p_3)S_v, \\
\frac{dE}{dt} &= (1-u_1(t))\lambda S_u + (1-u_2(t))(1-\theta)\lambda S_v \\
&\quad - (\mu + \sigma)E, \\
\frac{dI}{dt} &= \sigma(1-\gamma_1)E - (\mu + \delta + \alpha + \gamma_2)I, \\
\frac{dI_t}{dt} &= \sigma\gamma_1 E + \gamma_2 I - (\mu + u_3(t) + \tau)I_t, \\
\frac{dR}{dt} &= p_3 S_v + \alpha I + (u_3(t) + \tau)I_t - \mu R.
\end{aligned} \tag{46}$$

Currently, the following initial values of the state variables are assumed for biological reasons: Assuming $S_u(0) = S_u 0$, the following state variables also apply: $S_u 0 > 0, S_v 0, E0 > 0, I0 > 0, I_t 0 >$, and $R0 > 0$. Assuming t_f as the terminal time, we optimize the objective functional as follows.

$$\begin{aligned}
\mathcal{J}[x(t), u(t)] = \int_0^{t_f} \Big(& a_0 S_u(t) + a_1 E(t) + a_2 I(t) + a_3 I_t(t) \\
& + \frac{a_4}{2}u_1^2 + \frac{a_5}{2}u_2^2 + \frac{a_6}{2}u_3^2 \Big) \mathrm{d}t.
\end{aligned} \tag{47}$$

The final time is denoted by t_f. Finding the best control for u_1^*, u_2^*, and u_3^* is necessary such that

$$J(u_1^*, u_2^*, u_3^*) = min\{J(u_1^*, u_2^*, u_3^*) | u_1, u_2, u_3 \in U\}, \tag{48}$$

where the control set is $U = \{u_1^*, u_2^*, u_3^*\}$, such that u_1^*, u_2^*, u_3^* are measurable with $0 \le u_1^*, u_3^* \le 1$ and $0 \le u_2^* \le 0.9$ for $t \in [0, t_f]$. This is because, on average, vaccination programs should cover no more than approximately 90% of susceptible individuals. Now, the Hamiltonian is given by

$$\begin{aligned}
H = {} & a_0 S_u(t) + a_1 E(t) + a_2 I(t) + a_3 I_t(t) + \frac{a_4}{2}u_1^2 + \frac{a_5}{2}u_2^2 + \frac{a_6}{2}u_3^2 \\
& + \sum_{i=1}^{6} \lambda_i(t) f_i(t, S_u, S_v, E, I, I_t, R),
\end{aligned} \tag{49}$$

where $f_i(t, S_u, S_v, E, I, I_t, R)$ is the right-hand side of (46) and λ_i are the adjoint vectors.

$$\lambda : [0, t_f] \to \mathbb{R}^7, \lambda(t) = (\lambda_1(t), \lambda_2(t), \lambda_3(t), \lambda_4(t), \lambda_5(t), \lambda_6(t). \tag{50}$$

Considering the proper partial derivatives of the Hamiltonian (49) with respect to the related state variable, the system of equations can be constructed.

5.1. Existence of optimal control

Now, we prove that there is a solution for optimum control such that the objective functional J is minimized.

theorem. [35, 36]
An ideal control exists $u^* = (u_1^*, u_2^*, u_3^*)$ of the model (46), the control set piece-wise (48), objective functional (47) and the state solutions $(S_u^*, S_v^*, E^*, I^*, I_t^*, R^*)$ such that:

$$J(u^*) = \min_{\in U} J(u)$$

if each of the below circumstances is true:

- $\mathcal{Z} \neq \emptyset$ where $\mathcal{Z}$ is the initial conditions set in conjunction with the control u^*.
- U is closed and convex.
- $|f(t, x, u)| \le \chi_1|x| + \chi_2|u|$
- $g(t, x, u)$ in (47) is convex with respect to u.
- $g(t, x, u) \ge \chi_2|u|^\gamma - \chi_1$, where $\chi_1 > 0$ and $\chi_2 > 0$.

proof.

- The positivity and boundedness of model (2) were shown from Theorem 3.1. In contrast, the set of controls u is bounded, positive, and continuous, with $0 \le u \le 1$. A positive, bounded function is created by multiplying or combining two bounded, positive functions. This suggests that the control model, (46), is bounded and continuous. After careful consideration, we conclude that an initial condition with control u exists and is not empty. Consequently, the first condition is met.
- Recall that,

  $U = \{0 \le u_i(t) \le 1, i = 1, 2, 3$ and $t \in [0, t_f]$ and $u_i(t) : u_i(t)$ is Labesgue m

  Assume $u_1, u_3 \in U$ and $0 \le \alpha \le 1$ we therefore have,

  $$|\alpha u_1 + (1-\alpha)u_2| \le \alpha|u_1| + (1-\alpha)|u_2|, \tag{52}$$

  $\alpha u_1 \in U$ and $(1-\alpha)u_2 \in U$ are proof. This confirms that U is closed and convex. As a result, condition 2 is met.
- The matrix form of the control model (46) is as follows:

$$\begin{aligned}
f(t, x, u) = {} & \begin{bmatrix}
\Pi(1-p_1) - \lambda S_u - (\mu + p_2)S_u \\
\Pi p_1 + p_2 S - (1-\theta)\lambda S_v - (\mu + \omega + p_3)S_v \\
\lambda S_u + (1-\theta)\lambda S_v - (\sigma + \mu)E \\
\sigma(1-\gamma_1)E - (\mu + \delta + \alpha + \gamma_2)I \\
\sigma\gamma_1 E + \gamma_2 I - (\mu + \tau)I_t \\
p_3 S_v + \alpha I + \tau I_t - \mu R
\end{bmatrix} \\
& + \begin{bmatrix}
\lambda S_u & 0 & 0 \\
0 & (1-\theta)\lambda S_v & 0 \\
-\lambda S_u & -(1-\theta)\lambda S_v & 0 \\
0 & 0 & 0 \\
0 & 0 & -I_t \\
0 & 0 & I_t
\end{bmatrix}
\begin{bmatrix} u_1 \\ u_2 \\ u_3 \end{bmatrix}.
\end{aligned} \tag{53}$$

  With respect to the controls u_1, u_2, and u_3, (53) shows the RHS (right-hand side) linear dependence of the control model (46), where the coefficients are functions of time and state. The Jacobian matrix of (53) and $S \le N$ are responsible for the boundedness inequality.

$$\begin{aligned}
& |f(t, x, u)| \\
& \le \left\| \begin{bmatrix}
-\lambda - k_1 & \omega & 0 & -\frac{(1-\epsilon)\beta S_u}{N} & -\frac{(1-\epsilon)\beta S_u}{N} & 0 \\
p_2 & -(1-\theta)\lambda - k_2 & 0 & -\frac{(1-\epsilon)\beta(1-\theta)S_v}{N} & -\frac{(1-\epsilon)\beta(1-\theta)p_3 S_v}{N} & 0 \\
\lambda & (1-\theta)\lambda & -k_3 & \frac{(1-\epsilon)\beta(S_u + \eta(1-\theta)S_v)}{N} & \frac{\eta(1-\epsilon)\beta(S_u + (1-\theta)S_v)}{N} & 0 \\
0 & 0 & \sigma(1-\gamma_1) & -k_4 & 0 & 0 \\
0 & 0 & \sigma\gamma_1 & \gamma_2 & -k_5 & 0 \\
0 & p_3 & 0 & \alpha & \tau & -\mu
\end{bmatrix} \begin{bmatrix} S \\ S_u \\ S_v \\ E \\ I \\ I_t \\ R \end{bmatrix} \right\| \\
& + \left\| \begin{bmatrix}
\lambda S_u & 0 & 0 \\
0 & (1-\theta)\lambda S_v & 0 \\
-\lambda S_u & -(1-\theta)\lambda S_v & 0 \\
0 & 0 & 0 \\
0 & 0 & -I_t \\
0 & 0 & I_t
\end{bmatrix} \begin{bmatrix} u_1 \\ u_2 \\ u_3 \end{bmatrix} \right\|
\end{aligned} \tag{54}$$

  This demonstrates that in addition to the state and the bounded controls, $f(t, x, u)$ is bounded. The third criterion is satisfied.

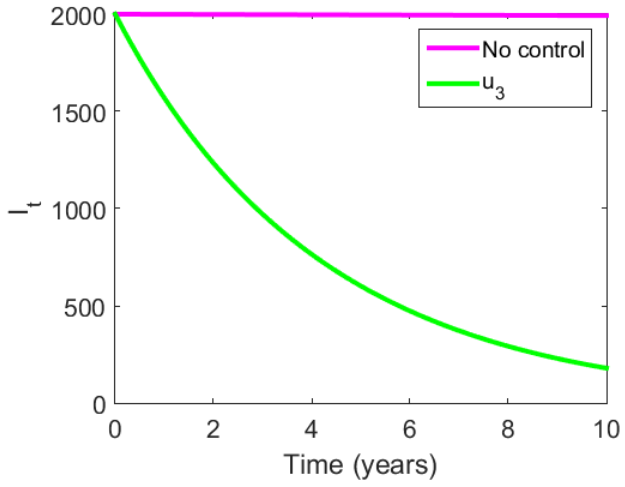

Figure 43. Influence of treatment control on infected individuals under treatment.

- In (47), the integrand function concerning u is quadratic. Since both the integrand and the quadratic function are convex, 4 holds.

$$\begin{aligned} g(t,x,u) &= a_0 S_u(t) + a_1 E(t) + a_2 I(t) + a_3 I_t(t) \\ &\quad + \frac{a_4}{2}u_1^2 + \frac{a_5}{2}u_2^2 + \frac{a_6}{2}u_3^2 \\ &\geq \frac{a_4}{2}u_1^2 + \frac{a_5}{2}u_2^2 + \frac{a_6}{2}u_3^2 \\ &\geq \frac{a_4}{2}u_1^2 + \frac{a_5}{2}u_2^2 + \frac{a_6}{2}u_3^2 - \frac{a_4}{2} \\ &= \min\left(\frac{a_4}{2}, \frac{a_5}{2}, \frac{a_6}{2}\right)(u_1^2 + u_2^2 + u_3^2) - \frac{a_4}{2} \\ &= \min\left(\frac{a_4}{2}, \frac{a_5}{2}, \frac{a_6}{2}\right)|u_1, u_2, u_3|^2 - \frac{a_4}{2} \end{aligned} \tag{55}$$

Let $\chi_1 = \frac{a_4}{2}, \chi_2 = \min\left(\frac{a_4}{2}, \frac{a_5}{2}, \frac{a_6}{2}\right)$ while $\nu = 2$, we have $g(t,x,u) \geq \chi_2|u_1,u_2,u_3|^\nu - \chi_1$ as expected.

Assuming that every prerequisite is met, u^* is the optimal control.

5.2. Pontryagin's maximum principle

Theorem. The related optimal state and the optimal solution u^* have adjoint variables λ_i $(i = 1...6)$. $S_u^*, S_v^*, E^*, I^*, I_t^*, R^*$ It reduced $J(u(t))$ above U so that

$$\begin{aligned} \frac{d\lambda_1}{dt} &= -a_0 + \lambda_1 k_1 + (\lambda_1 - \lambda_3)\frac{(1-u_1)(1-\epsilon)\beta(I+\eta I_t)(N-S_u)}{N^2} - \lambda_2 p_2, \\ \frac{d\lambda_2}{dt} &= -\lambda_1\omega + k_2\lambda_2 + \frac{(\lambda_2-\lambda_3)(1-\theta)(1-u_2)(1-\epsilon)\beta(I+\eta I_t)(N-S_v)}{N^2} - \lambda_6 p_3, \\ \frac{d\lambda_3}{dt} &= -a_1 + \lambda_3 k_3 - \lambda_4\sigma(1-\gamma_1) - \lambda_5\sigma\gamma_1, \\ \frac{d\lambda_4}{dt} &= -a_2 + \frac{(\lambda_1-\lambda_3)(1-u_1)(1-\epsilon)\beta S_u(N-I)}{N^2} \\ &\quad + \frac{(\lambda_2-\lambda_3)(1-\theta)(1-u_2)(1-\epsilon)\beta S_v(N-I)}{N^2} \\ &\quad + \lambda_4 k_4 - \lambda_5\gamma_2 - \lambda_6\alpha, \\ \frac{d\lambda_5}{dt} &= -a_3 + \frac{(\lambda_1-\lambda_2)(1-u_1)(1-\epsilon)\beta\eta S_u(N-I_t)}{N^2} \\ &\quad + \frac{(\lambda_2-\lambda_3)(1-\theta)(1-u_2)(1-\epsilon)\beta\eta S_v(N-I_t)}{N^2} \\ &\quad - \lambda_5(-u_3+k_5) - \lambda_6(u_3-\tau), \\ \frac{d\lambda_6}{dt} &= \mu\lambda_6, \end{aligned} \tag{56}$$

and the transversality condition $\lambda_i(t_f) = 0$, in which $i = 1...7$. Furthermore,

$$u_1^* = \min\left(\max\left(0, \frac{(\lambda_1-\lambda_3)(1-\epsilon)\beta(I+\eta I_t)S_u}{a_4 N}\right), 1\right), \tag{57}$$

$$u_2^* = \min\left(\max\left(0, \frac{(\lambda_2-\lambda_3)(1-\epsilon)\beta(I+\eta I_t)S_v}{a_5 N}\right), 1\right), \tag{58}$$

$$u_3^* = \min\left(\max\left(0, \frac{I_t(\lambda_5-\lambda_6)}{a_6}\right), 1\right). \tag{59}$$

Proof. . Pontryagin's Principle is used to find the adjoint variables and control functions (transversality condition).

$$\begin{aligned} H &= a_0 S_u(t) + a_1 E(t) + a_2 I(t) + a_3 I_t + \frac{a_4}{2}u_1^2 + \frac{a_5}{2}u_2^2 + \frac{a_6}{2}u_3^2 \\ &\quad + \sum_{i=1}^{6}\lambda_i(t) f_i(t, S_u, S_v, E, I, I_t, R) \end{aligned} \tag{60}$$

$$\begin{aligned} &= a_0 S_u + a_1 E + a_2 I + a_3 I_t + 1/2\, a_4 {u_1}^2 + 1/2\, a_5 {u_2}^2 + 1/2\, a_6 {u_3}^2 \\ &+ \lambda_1\left(\Pi(1-p_1) + \omega S_v - \frac{(1-u_1)(1-\epsilon)\beta(I+\eta I_t)S_u}{N} - k_1 S_u\right) \\ &+ \lambda_2\left(\Pi p_1 + p_2 S_u - \frac{(1-\theta)(1-u_2)(1-\epsilon)\beta(I+\eta I_t)S_v}{N} - k_2 S_v\right) \\ &+ \lambda_3\left(\frac{(1-u_1)(1-\epsilon)\beta(I+\eta I_t)S_u}{N} + \frac{(1-\theta)(1-u_2)(1-\epsilon)\beta(I+\eta I_t)S_v}{N} - k_3 E\right) \\ &+ \lambda_4(\sigma(1-\gamma_1)E - k_4 I) \\ &+ \lambda_5(\sigma\gamma_1 E + \gamma_2 I - (u_3+k_5)I_t) \\ &+ \lambda_6(p_3 S_v + \alpha I + (u_3+\tau)I_t - \mu R). \end{aligned} \tag{61}$$

Following the differentiation of Hamiltonian (61) with respect to the adjoint variables or state variables, we obtain

$$\begin{aligned} \frac{d\lambda_1}{dt} &= -\frac{\partial H}{\partial S_u} = -a_0 + \lambda_1 k_1 + (\lambda_1-\lambda_3)\frac{(1-u_1)(1-\epsilon)\beta(I+\eta I_t)(N-S_u)}{N^2} \\ &\quad - \lambda_2 p_2, \\ \frac{d\lambda_2}{dt} &= -\frac{\partial H}{\partial S_v} = -\lambda_1\omega + k_2\lambda_2 + (\lambda_2-\lambda_3)(1-\theta)(1-u_2)(1-\epsilon) \\ &\quad \times \frac{\beta(I+\eta I_t)(N-S_v)}{N^2} - \lambda_6 p_3, \\ \frac{d\lambda_3}{dt} &= -\frac{\partial H}{\partial E} = -a_1 + \lambda_3 k_3 - \lambda_4\sigma(1-\gamma_1) - \lambda_5\sigma\gamma_1, \\ \frac{d\lambda_4}{dt} &= -\frac{\partial H}{\partial I} = -a_2 + \frac{(\lambda_1-\lambda_3)(1-u_1)(1-\epsilon)\beta S_u(N-I)}{N^2} \\ &\quad + \frac{(\lambda_2-\lambda_3)(1-\theta)(1-u_2)(1-\epsilon)\beta S_v(N-I)}{N^2} \\ &\quad + \lambda_4 k_4 - \lambda_5\gamma_2 - \lambda_6\alpha, \\ \frac{d\lambda_5}{dt} &= -\frac{\partial H}{\partial I_t} = -a_3 + \frac{(\lambda_1-\lambda_2)(1-u_1)(1-\epsilon)\beta\eta S_u(N-I_t)}{N^2} \\ &\quad + \frac{(\lambda_2-\lambda_3)(1-\theta)(1-u_2)(1-\epsilon)\beta\eta S_v(N-I_t)}{N^2} \\ &\quad - \lambda_5(-u_3+k_5) - \lambda_6(u_3-\tau), \\ \frac{d\lambda_6}{dt} &= -\frac{\partial H}{\partial R} = \mu\lambda_6. \end{aligned} \tag{62}$$

Using the optimality criteria provided with respect to the adjoint variables and ideal circumstances, we may determine the control u^*.

$$\frac{\partial H}{\partial u_i} = 0, i = 1, 2, 3. \tag{63}$$

$$u_1^* = \min\left(\max\left(0, \frac{(\lambda_1-\lambda_3)(1-\epsilon)\beta(I+\eta I_t)S_u}{a_4 N}\right), 1\right), \tag{64}$$

$$u_2^* = \min\left(\max\left(0, \frac{(\lambda_2 - \lambda_3)(1-\epsilon)\beta(I+\eta I_t)S_v}{a_5 N}\right), 1\right), \tag{65}$$

$$u_3^* = \min\left(\max\left(0, \frac{I_t(\lambda_5 - \lambda_6)}{a_6}\right), 1\right). \tag{66}$$

6. Numerical simulations

The numerical simulation of the model state variables is shown in this section using the parameter values listed in Table 2. A numerical simulation is carried out to get a thorough grasp of the transmission dynamics of the model (2). The behaviour of the compartments and the ways in which important factors affect the state variables are shown using time series graphs.

6.1. Optimal control simulation

In this subsection, the control profile of the three controls and their influence on the compartments that are expected to be minimized will be tested.

6.2. Simulated results and discussion

Figure 6 shows the influence of awareness on infected individuals receiving treatment. Figures 7, 8, 9, 10, 11, and Figure 12 show how the state variables of the model (2) behave. Figure 13 describes the impact of vaccination at recruitment on exposed individuals, varying vaccination rates at recruitment, and shows no impact on exposed individuals. Figure 14 describes the impact of vaccination in recruitment in infectious individuals, varying vaccination rates at recruitment, and shows no impact on infectious individuals. Figure 15 describes the impact of vaccination at recruitment on infectious individuals under treatment, varying vaccination rates at recruitment, showing no impact on infectious individuals under treatment. Figure 16 describes the impact of vaccination due to awareness in exposed individuals, varying vaccinations due to awareness causes exposed individuals to decrease, this shows that vaccination due to awareness has an impact on exposed individuals. Figure 17 describes the impact of vaccination due to awareness on infectious individuals, varying vaccinations due to awareness causes the infectious individuals to decrease slightly; this shows that vaccination due to awareness has little impact on infectious individuals. Figure 18 describes the impact of vaccination due to awareness on infectious individuals under treatment, varying vaccination due to awareness causes the infectious individuals under treatment to decrease slightly, this shows that vaccination due to awareness has little impact on infectious individuals under treatment.

Figure 19 describes the impact of vaccination boosters on exposed individuals, varying vaccination boosters show little impact on exposed individuals. Figure 20 describes the impact of vaccination boosters on infectious individuals, varying vaccination boosters show little impact on infectious individuals. Figure 21 describes the impact of vaccination boosters on infectious individuals under treatment, and varying vaccination boosters do not have an impact on infectious individuals under treatment. Figure 22 describes the impact of awareness in exposed individuals, varying vaccination awareness rates cause exposed individuals to decrease drastically, which shows that awareness has much impact on exposed individuals. Figure 23 describes the impact of awareness on infectious individuals, varying awareness makes infectious individuals decrease greatly, this shows that awareness has a significant impact on infectious individuals. Figure 24 describes the impact of awareness on infectious individuals under treatment, varying awareness rates make infectious individuals under treatment decrease; this shows that awareness has an impact on infectious individuals under treatment.

Figure 25 describes the impact of treatment due to awareness of exposed individuals on exposed individuals, varying treatment due to awareness of exposed individuals, shows a great impact on exposed individuals. Figure 26 describes the impact of treatment due to awareness of the exposed individuals on infectious individuals, varying treatment due to awareness of the exposed individuals shows much impact on infectious individuals. Figure 27 describes the impact of treatment due to awareness of the exposed individuals on infectious individuals under treatment, varying treatment due to awareness of the exposed individuals, shows a significant impact on infectious individuals under treatment. Figure 28 describes the impact of treatment due to awareness of infectious individuals on exposed individuals, varying treatment due to awareness of the infectious individuals rate makes exposed individuals drastically decrease, this shows that treatment due to awareness of infectious individuals has much impact on exposed individuals. Figure 29 describes the impact of treatment due to awareness of infectious individuals on infectious individuals, varying treatment due to awareness of infectious individuals makes the infectious individuals decrease greatly, which shows that treatment due to awareness of infectious individuals has a much impact on infectious individuals. Figure 30 describes the impact of treatment due to awareness of infectious individuals on infectious individuals under treatment, varying treatment due to awareness of the rate infectious individuals rate, makes the infectious individuals under treatment decrease, this shows that treatment due to awareness of infectious individuals has a significant impact on infectious individuals under treatment.

Figure 31 describes the profile of the three controls proposed in the model (46). Figure 32 describes when there is no control and when there is only health education control on un-vaccinated susceptible individuals when there is no control, the un-vaccinated individual's population is steady, but if health education control is introduced the population keeps declining as time goes on. Figure 33 describes when there is no control and when there are only controls of health education in exposed individuals. When there is no control, the exposed individual's population reduces to increase after some time, but if health education control is introduced, the population keeps declining to almost zero. Figure 34 describes when there is no control and when there are only controls of health education in infected individuals. When there is no control, the population of the infected individuals increases unboundedly, but if control of health education is introduced, the population decreases. Figure 35 describes when there is no control and when there are only controls of health education in infected individuals under treatment, when there is no control, the infected individuals under treatment population is steady but if health education control is introduced, the population keeps declining drastically as time goes on. Figure 36 describes when there is no control and when there is only vaccination control on un-vaccinated susceptible individuals. When there is no control, the un-vaccinated individual's population is steady, but if vaccination control is introduced the population keeps declining as time goes on. Figure 37 describes when there is no control and when there is only vaccinated control on exposed individuals. When there is no control, the population of the exposed individuals decreases to increase after some time, but if vaccination control is introduced, the population keeps declining to almost zero. Figure 38 describes when there is no control and when there is only vaccination control on infected individuals. When there is no control, the infected individual's population increases unboundedly but if vaccination control is introduced, the population decreases a little. Figure 39 describes when there is no control and when there is only vaccination control on infected individuals under treatment, when there is no control, infected

individuals under treatment population are steady, but if vaccination control is introduced, the population continues to decline drastically as time goes on.

Figure 40 describes when there is no control and when there is only treatment control on un-vaccinated susceptible individuals. When there is no control, the un-vaccinated individual's population is steady but if treatment control is introduced the population keeps declining as time goes on. Figure 41 describes when there is no control and when there is only treatment control on exposed individuals, when there is no control, the population of the exposed individual decreases and increases after some time, but if vaccination control is introduced, the population declines a little. Figure 42 describes when there is no control and when there is only treatment control on infected individuals. When there is no control, the infected individual's population increases unboundedly but if treatment control is introduced, the population decreases significantly. Figure 43 describes when there is no control and when there is only treatment control on infected individuals under treatment, when there is no control, infected individuals under treatment population are steady, but if treatment control is introduced, the population continues to decline drastically as time goes on.

7. Conclusion and recommendation

A mathematical model of pertussis has been formulated, considering the effect of combining awareness with vaccination simultaneously. We assess the positivity and boundedness of the proposed model. The threshold quantity has been computed. The local stability of the disease-free equilibrium has also been evaluated, as well as the global stability. The existence of endemic equilibrium points has been ascertained, and the global stability of endemic equilibrium points has been assessed. The proposed model fits real data on pertussis in Austria, which shows that the proposed model fits the data. Furthermore, sensitivity analysis of all parameters of the proposed model has been tested on the control reproduction number, which shows that awareness rate is the most sensitive parameter in reducing the control reproduction number and the most sensitive parameter in increasing the reproduction number is the effective contact rate. Numerical simulation reveals that awareness is the most influential parameter in reducing infection in the population. In addition, vaccination and treatment are very important in controlling pertussis in society. Optimal control analysis showed that health education and vaccination are very important in controlling pertussis in society. We therefore recommend this model for the government, health providers, and nongovernmental organizations to consider the results of this research, it will help to control pertussis in the environment.

References

[1] B. Surmann, J. Witte, M. Batram, C. P. Criee, C. Hermann, A. Leischker, J. Schelling, M. Steinmüller, K. Wahle, A. F. Heiseke & P. Marijic, "Epidemiology of Pertussis and Pertussis-Related Complications in Adults: A German Claims Data", Infectious Diseases and Therapy **13** (2024) 385. https://doi.org/10.1007/s40121-023-00912-z.

[2] M. Korppi, "Coqueluche: ainda um desafio", Jornal de Pediatria **89** (2013) 520. https://doi.org/10.1016/j.jped.2013.09.001.

[3] P. Pesco, P. Bergero, G. Fabricius, & D. Hozbor, "Modelling the effect of changes in vaccine effectiveness and transmission contact rates on pertussis epidemiology", Epidemics **7** (2014) 13. https://doi.org/10.1016/j.epidem.2014.04.001.

[4] M. Suleman & S. Riaz, "An optimal control of vaccination applied to whooping cough model", Punjab University Journal of Mathematics **51** (2020) 121. https://pu.edu.pk/images/journal/maths/PDF/Paper-9_51_5_2019.pdf.

[5] M. M. Alqarni, A. Nasir, M. A. Alyami, A. Raza, J. Awrejcewicz, M. Rafiq, N. Ahmed, T. Sumbal Shaikh & E. E. Mahmoud, "A SEIR Epidemic Model of Whooping Cough-Like Infections and Its Dynamically Consistent Approximation", Complexity **2022** (2022) 3642444. https://doi.org/10.1155/2022/3642444.

[6] Immunization, Vaccines and Biologicals, by World Health Organization, (2024). https://www.who.int/teams/immunization-vaccines-and-biologicals.

[7] A. I. K. Butt, "Atangana-Baleanu fractional dynamics of predictive whooping cough model with optimal control analysis", Symmetry **15** (2023) 1773. https://doi.org/10.3390/sym15091773.

[8] Y. H. Choi, H. Campbell, G. Amirthalingam, A. J. Van Hoek & E. Miller, "Investigating the pertussis resurgence in England and Wales, and options for future control", BMC Medicine **14** (2016) 1. https://doi.org/10.1186/s12916-016-0665-8.

[9] National Centre for Immunization and Respiratory Diseases, by Centre for Disease Control and Prevention, (2024). https://www.cdc.gov/ncird/index.html.

[10] Immunization program data: regional and country, by World Health Organization, (2022). https://www.who.int/publications/i/item/9789290619802.

[11] Nigeria Centre for Disease Control and Prevention (2011). https://ncdc.gov.ng/.

[12] A. C. Freitas, V. Okano & J. C. R. Pereira, "Pertussis booster vaccine for adolescents and young adults in São Paulo, Brazil", Revista de Saude Publica **45** (2011) 1162. https://doi.org/10.1590/s0034-89102011000600008.

[13] D. Jayasundara, E. Lee, S. Octavia, R. Lan, M. M. Tanaka, & J. G. Wood, "Emergence of pertactin-deficient pertussis strains in Australia can be explained by models of vaccine escape", *Epidemics* **31** (2020) 100388. https://doi.org/10.1016/j.epidem.2020.100388.

[14] A. A. Yakubu, F. A. Abdullah, A. I. M. Ismail & Y. M. Yatim, "Global stability analysis of pertussis transmission dynamics with maternally derived immunity compartment", AIP Conference Proceedings **2423** (2021). https://doi.org/10.1063/5.0073271.

[15] E. Yaylali, J. S. Ivy, R. Uzsoy, E. Samoff, A. M. Meyer & J. M. Maillard, "Modeling the effect of public health resources and alerting on the dynamics of pertussis spread", Health Systems **5** (2016) 81. https://doi.org/10.1057/hs.2015.6.

[16] P. Misra & D. K. Mishra, "Modelling the effect of booster vaccination on the transmission dynamics of diseases that spread by droplet infection", Nonlinear Analysis: Hybrid Systems **3** (2009) 657. https://doi.org/10.1016/j.nahs.2008.10.002.

[17] M. van Boven, H. E. de Melker, J. F. Schellekens, & M. Kretzschmar, "Waning immunity and sub-clinical infection in an epidemic model: implications for pertussis in The Netherlands", Mathematical Biosciences **164** (2000) 161. https://doi.org/10.1016/s0025-5564(00)00009-2.

[18] L. Mamadou Diagne, F. B. Agusto, H. Rwezaura, J. M. Tchuenche & S. Lenhart, "Optimal control of an epidemic model with treatment in the presence of media coverage", Scientific African **24** (2024) e02138. https://doi.org/10.1016/j.sciaf.2024.e02138.

[19] A. Stuart & A. R. Humphries, *Dynamical Systems and Numerical Analysis*, Vol. 2, Cambridge University Press, Cambridge, UK, 1998. https://assets.cambridge.org/97805214/96728/frontmatter/9780521496728_frontmatter.pdf.

[20] U. T. Mustapha, A. Ado, A. Yusuf, S. Qureshi & S. S. Musa, "Mathematical dynamics for HIV infections with public awareness and viral load detectability", Mathematical Modelling and Numerical Simulation with Applications, **3** (2023) 256. https://doi.org/10.53391/mmnsa.1349472.

[21] G. Djatcha Yaleu, S. Bowong, E. Houpa Danga & J. Kurths, "Mathematical analysis of the dynamical transmission of Neisseria meningitidis serogroup A", International Journal of Computer Mathematics **94** (2017) 2409. http://dx.doi.org/10.1080/00207160.2017.1283411.

[22] P. Van De Driessche & J. Watmough, "Reproduction number and subthreshold endemic equilibrium for compartmental models of disease transmission", Mathematical Biosciences **180** (2002) 29. https://doi.org/10.1016/s0025-5564(02)00108-6.

[23] Y. U. Ahmad, J. Andrawus, A. Ado, Y. A. Maigoro, A. Yusuf, S. Althobaiti & U. T. Mustapha, "Mathematical modeling and analysis of human-to-human monkeypox virus transmission with post-exposure vaccination", Modeling Earth Systems and Environment **10** (2024) 2711.

https://doi.org/10.1007/s40808-023-01920-1.

[24] J. Andrawus, A. Yusuf, U. T. Mustapha, A. S. Alshom-rani & D. Baleanu, "Unravelling the dynamics of Ebola virus with contact tracing as control strategy", Fractals, **31** (2023) 2340159. https://doi.org/10.1142/S0218348X2340159X.

[25] J. Andrawus, A. I. Muhammad, B. A. Denue, A. Yusuf & S. Salahshour, "Unraveling the importance of early awareness strategy on the dynamics of drug addiction using mathematical modeling approach", Chaos: An Interdisciplinary Journal of Nonlinear Science, **34** (2024). https://doi.org/10.1063/5.0203892.

[26] O. Johnson & H. O. S. Edogbanya, "Mathematical modeling for mitigating pertussis resurgence in the post-COVID-19 era: A sensitivity analysis and intervention strategies", International Journal of Novel Research in Physics Chemistry & Mathematics **11** (2024) 12. https://doi.org/10.5281/zenodo.10721146.

[27] Annual Epidemiological Report pertussis, by European Center of Disease Control, (2022). https://www.ecdc.europa.eu/sites/default/files/documents/PERT_AER_2022_Report.pd.

[28] J. P. Lasalle, *The stability of dynamical systems*, Regional conference series in applied mathematics, SIAM, Philadelphia, 1976. https://epubs.siam.org/doi/pdf/10.1137/1.9781611970432.bm.

[29] R. Craig, E. Kunkel, N. S. Crowcroft, M. C. Fitzpatrick, H. De Melker, B. M. Althouse & S. Bolotin, "Asymptomatic infection and transmission of pertussis in households: A systematic review", Clinical Infectious Diseases **70** (2020) 152. https://doi.org/10.1093/cid/ciz531.

[30] P. M. Luz, C. T. Codeço, G. L. Werneck & C. J. Struchiner, "A modelling analysis of pertussis transmission and vaccination in Rio de Janeiro, Brazil", Epidemiology, **134** (2006) 850. https://doi.org/10.1017/S095026880500539X.

[31] U. T. Mustapha, A. I. Muhammad, A. Yusuf, N. Althobaiti, A. I. Aliyu & J. Andrawus, "Mathematical dynamics of meningococcal meningitis: Examining carrier diagnosis and prophylaxis treatment", International Journal of Applied and Computational Mathematics **11** (2025) 77. https://doi.org/10.1007/s40819-025-01890-1.

[32] K. G. Ibrahim, J. Andrawus, A. Abubakar, A. Yusuf, S. I. Maiwa, K. Bitrus, M. Sani, I. Abdullahi, S. Babuba & J. Jonathan, "Mathematical analysis of chickenpox population dynamics unveiling the impact of booster in enhancing recovery of infected individuals", Modeling Earth Systems and Environment **11** (2025) 1. https://doi.org/10.1007/s40808-024-02219-5.

[33] J. Andrawus, A. Abubakar, A. Yusuf, A. A. Andrew, B. Uzun & S. Salahshour, "Impact of public awareness on haemo-lyphatic and meningo-encepphalitic stage of sleeping sickness using mathematical model approach", European Physical Journal Special Topics (2024) 1. https://doi.org/10.1140/epjs/s11734-024-01417-7.

[34] J. Andrawus, Y. U. Ahmad, A. A. Andrew, A. Yususf, S. Qureshe, B. Akawu, H. Abdul & S. Salahshour, "Impact of surveillance in human-to-human transmission of monkeypox virus", The European Physical Journal Special Topics (2024) 1. https://doi.org/10.1140/epjs/s11734-024-01346-5.

[35] B. Heimann, W. H. Fleming & R. W. Rishel, "Deterministic and stochastic optimal control", Zeitschrift f"ur Angewandte Mathematik und Mechanik **59** (1979) 494. https://doi.org/10.1002/zamm.19790590940.

[36] J. Andrawus, S. Abdulrahman, R. V. K. Singh & S. S. Manga, "Optimal control of mathematical modelling for Ebola virus population dynamics in the presence of vaccination", DUJOPAS **8** (2022) 126. https://doi.org/10.4314/dujopas.v8i1b.15.